of Hb absorbance. However, the measured Hb concentration in the LEH solution, as determined by the Erma PCE 170 hematology analyzer, was 5-fold higher than the actual concentration that was determined when using a specific enzyme-linked immunosorbent assay for human Hb during the production of LEH (see Figure, Supplemental Digital Content 1, http://links.lww.com/SHK/A51). We then estimated the actual Hb concentration in the LEH-transfused mouse samples based on the measured Hb concentration of each sample. First, the mouse RBC–derived Hb concentration in an LEH-mixed blood sample was estimated by reproducing an RBC suspension that had the same hematocrit as the sample. We then measured its Hb concentration, because the hematocrit in the LEH-mixed blood sample reflected the concentration of the mouse RBCs, given that the mean corpuscular volume essentially remained unchanged in all of the mice during the experiment. The LEH-derived Hb concentration was then obtained by subtracting the mouse RBC–derived Hb concentration from the measured Hb concentration, with the determination of the actual LEH-derived Hb concentration calculated by dividing the obtained LEH-derived Hb concentration by 5. The total concentration of Hb in the samples containing a mixture of RBCs and LEH was determined by adding the estimated LEH-derived Hb concentration and the mouse RBC–derived Hb concentration (12).

Measurements of plasma NO_2^-, NO_3^-, TNF, and erythropoietin levels

Collected blood samples were immediately heparinized and then centrifuged at 50,000*g* at 4°C for 20 min to remove the LEH particles. The plasma supernatant was stored at −80°C until assay. For NO determination, the plasma was mixed with methanol (1:1) followed by centrifugation at 10,000*g* at 4°C for 10 min to remove proteins, and the supernatant was used for measurement of plasma NO_2^- and NO_3^- levels. Determinations of plasma NO levels were performed on a high-performance liquid chromatography–Griess system (ENO-20; Eicom, Kyoto, Japan). This instrument applied a post-column derivatization method with Griess reagent for nitrite and nitrate detection. At first, nitrite and nitrate are separated from the other substances on a separation column. Thereafter, nitrite reacts with the Griess reagent and generates diazo compounds. The separated nitrate is reduced by a cadmium-copper column to react with the Griess reagent. The level of diazo compounds is then measured by a visible detector installed in a column oven at high stability and sensitivity. The detection limits and sensitivities were 0.01 μM for both NO_2^- and NO_3^-. The loading volume of plasma was 10 μL. The area under the curve of each chromatogram was calculated for quantitative analysis of NO_2^- and NO_3^-, using the analyzing software PowerChrom (AD Instrument Co, Ltd, Tokyo, Japan).Plasma samples were also tested with enzyme-linked immunosorbent assay kits for TNF (BD Pharmingen) and mouse Epo immunoassay (R&D Systems).

Operation procedure and samples analysis

All operations are performed with a microscope (SZ6045; Olympus Optical, Tokyo, Japan) and microsurgical technique. If the failure of the first fluid resuscitation or technical problems were found, the samples were removed from the data. The reason of failure was mainly unexpected bleeding or extravasation such as intramuscular infusion or subcutaneous infusion.

Statistical analysis

Statistical analyses were performed using the Stat View 4.02J software package (Abacus Concepts, Berkeley, Calif). Survival rates were compared by the Wilcoxon signed rank test. Statistical evaluations between two groups were compared using the Student *t* test, and any other statistical evaluations were compared using one-way ANOVA, followed by the Bonferroni post hoc test. Data are presented as the mean ± SE. $P < 0.05$ was considered to be statistically significant.

RESULTS

Fatal hypohemoglobinemia induced by blood exchange

Blood exchange was performed on mice (n = 15) by a 0.2-mL blood withdrawal and an isovolumetric intravenous injection of 5% albumin. The mice repeatedly received this blood exchange until they died. No mice survived beyond eight iterations of this blood exchange (Fig. 2A). Mean arterial pressure was decreased to 40 mmHg in the mice after seven exchanges of blood (Fig. 2B), and Hb concentration was decreased to approximately 5 g/dL because of progressive hemodilution, suggesting a fatal hypohemoglobinemia (Fig. 2C). Hematocrit, RBC count, platelet, and WBC counts were also decreased with hemodilution (Fig. 2, D–G).

Resuscitation of fatal hypohemoglobinemia by intravenous transfusion with LEH or RBCs

After seven exchanges of blood, the mice were intravenously transfused with 0.5 mL LEH (n = 20), 5% albumin (n = 20), or washed RBCs (n = 20). Although no mice were rescued by albumin transfusion, all of the LEH- and RBC-transfused mice recovered from hypohemoglobinemia within 6 h (normally fatal), suggesting a success in initial resuscitation (Fig. 3A). Both transfusions with LEH and RBCs promptly restored MAP to 70 mmHg from 30 mmHg. Nevertheless, the survival rate of LEH-transfused mice gradually decreased to 25% at 36 h, whereas RBC-transfused mice sustained a higher survival rate (Fig. 3A). Both LEH-transfused and RBC-transfused mice showed an increase in Hb concentration immediately after transfusion (at 5 min) (Fig. 3B). However, LEH-transfused mice did not show an increase in hematocrit or

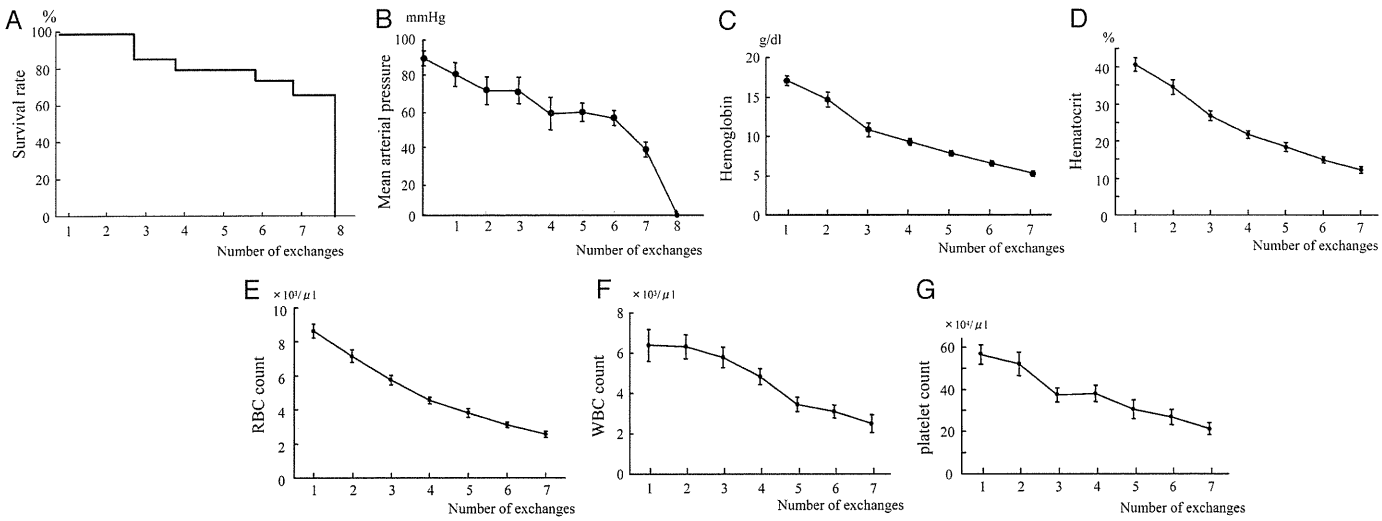

FIG. 2. **Data on the survival (A), mean arterial pressure (B), Hb level (C), hematocrit (D), RBC count (E), WBC count (F), and platelet count (G) of mice undergoing progressive hemodilution.** The mice repeatedly had 0.2 mL of blood withdrawn followed by isovolumetric intravenous injection with 5% albumin. Data are mean ± SE from 15 mice.

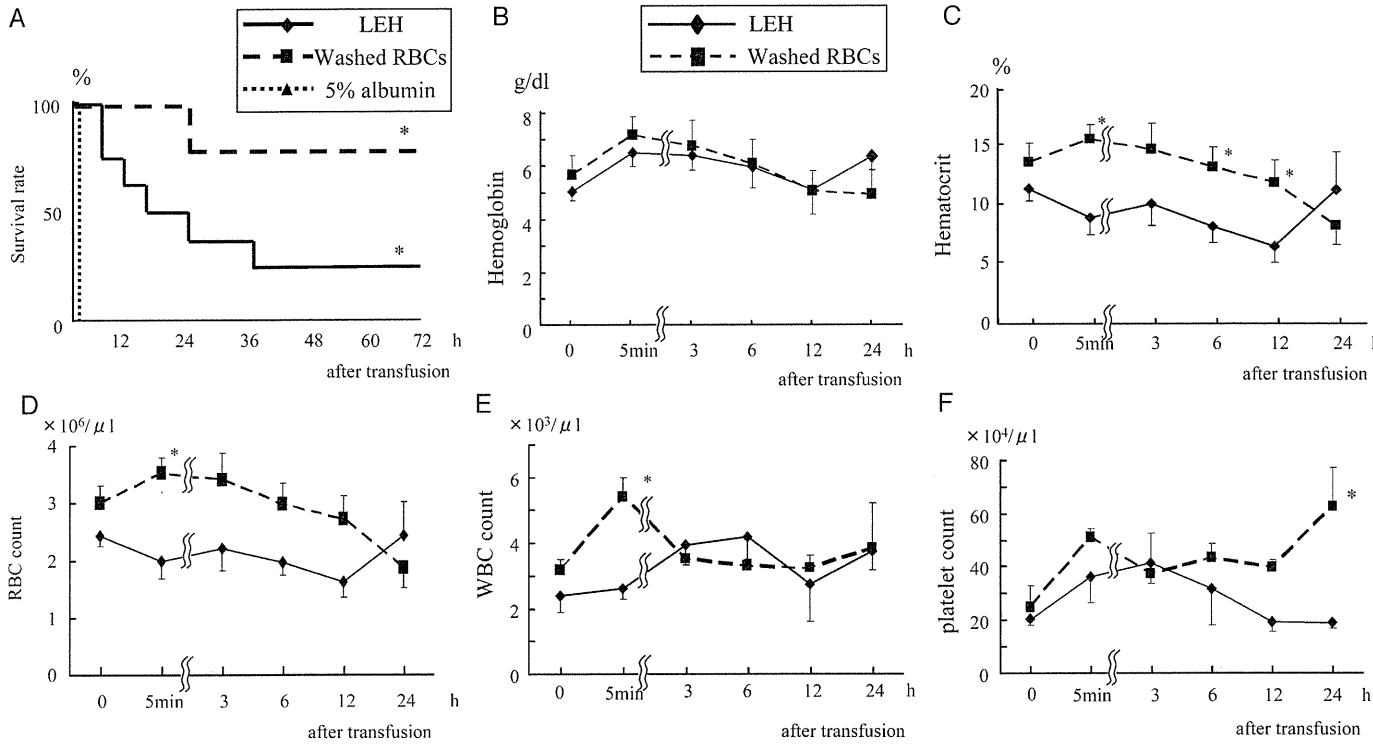

FIG. 3. **The effect of resuscitation fluid on the survival (A), Hb level (B), hematocrit (C), RBC count (D), WBC count (E), and platelet count (F) in mice with fatal hypohemoglobinemia.** Fatal hypohemoglobinemia was induced in the mice by seven 0.2-mL exchanges of blood. Thereafter, the mice were treated by intravenous transfusion with 0.5 mL LEH, 5% albumin, or washed RBCs. Data are mean ± SE from 20 mice in each group. $*P < 0.05$ vs. the other groups.

RBC count after transfusion (although RBC-transfused mice did), because the present hematology analyzer cannot detect a vesicle the size of LEH (200 nm) (Fig. 3, C and D). White blood cell count was transiently increased in the mice immediately after RBC transfusion but not after LEH transfusion (Fig. 3E). The platelet count was also increased 24 h after RBC transfusion but not after LEH transfusion (Fig. 3F). These findings suggest the possibility that hematologic alterations induced by massive blood transfusion do not occur after massive LEH transfusion.

Serum TNF and plasma NO levels after resuscitation by intravenous transfusion with LEH or RBCs

Serum TNF levels were increased in the mice with repeated blood exchanges, whereas those levels decreased after transfusion with either RBCs or LEH (Fig. 4A); no statistical difference in the change in TNF levels was observed between the two groups. Although plasma NO_2^- levels were not increased in the mice during the blood exchanges, they were promptly increased after RBC transfusion. Plasma NO_2^- levels also gradually increased in the mice after LEH transfusion, but the increase was quite different from that after RBC transfusion (Fig. 4B). However, no obvious decrease in the plasma NO_2^- levels was observed after LEH transfusion. Plasma NO_3^- levels were slightly decreased in both groups not only during the blood exchanges but also after RBC transfusion (Fig. 4C). These findings suggest that LEH transfusion does not induce a potent NO scavenging effect in the subject mice.

The effect of additional intravenous LEH or washed RBC transfusion after first intravenous transfusion

We examined the effect of additional intravenous LEH transfusions (n = 20) or washed RBC transfusions (n = 10) 6 h after first transfusion. Twenty percent of the mice died within

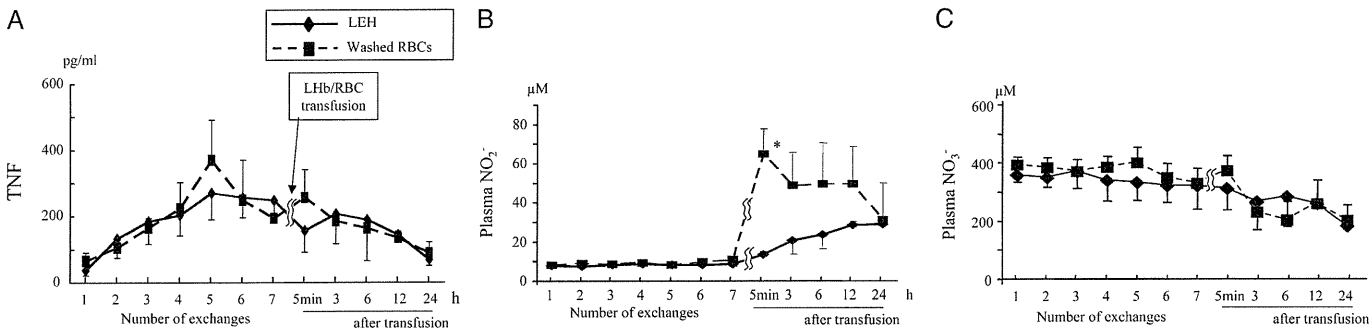

FIG. 4. **The change in serum TNF (A), plasma NO_2^- (B), and NO_3^- (C) levels in the mice during the blood exchanges and after resuscitation by LEH or washed RBC transfusions, as described in Figure 2.** Data are mean ± SE from 10 mice in each group. $*P < 0.05$ vs. the other group.

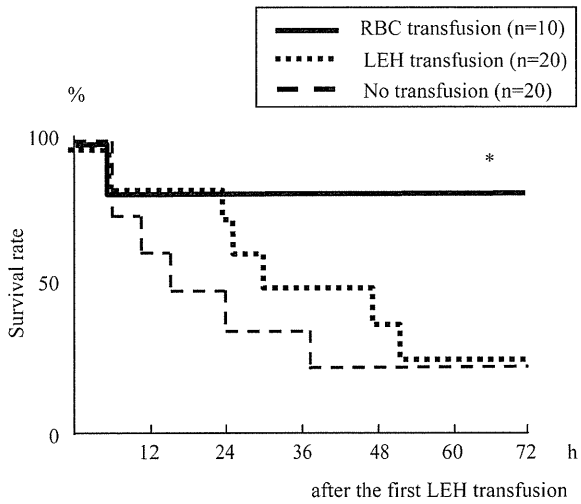

FIG. 5. **Survival of repeated LEH transfusion and RBC transfusion after LEH transfusion in mice with fatal hypohemoglobinemia.** Fatal hypohemoglobinemia was induced in the mice by seven 0.2-mL exchanges of blood. Thereafter, the mice were treated by intravenous transfusion with 0.5 mL LEH or washed RBCs 6 h after intravenous transfusion with 0.5 mL LEH. Data are mean ± SE in each group. $*P < 0.05$ vs. the other groups.

6 h and did not receive LEH or washed RBC transfusion. The remained mice all survived after an additional washed RBC administration. The survival of mice receiving an additional LEH transfusion extended to 24 h, but the survival rate had decreased to same level as a single LEH administration at 48 h (Fig. 5).

Resuscitation of massive hemorrhage model by intraosseous transfusion with LEH or RBCs

Mice had 0.8 mL of blood withdrawn and subsequently were intraosseously infused with 1 mL of 5% albumin. All subjected mice survived the first hemorrhage with this treatment, although no mice survived without any fluid resuscitation. Next, those mice had 0.3 mL of additional blood withdrawn and then were intraosseously transfused with 1 mL of either LEH (n = 10), 5% albumin (n = 10), or RBCs (n = 10). Immediately after the second withdrawal, Hb concentration was decreased to approximately 6 g/dL in the subject mice, suggesting a severe hypohemoglobinemia. Intraosseous infusion with 5% albumin rescued approximately 30% of the subjected mice after the second withdrawal; however, intraosseous transfusion with LEH significantly increased mouse survival (Fig. 6A). Unexpectedly, intraosseous transfusion with RBCs did not effectively increase mouse survival (Fig. 6A). These results suggest the following two important findings. First, intraosseous transfusion with RBCs may not be effective for serious massive hemorrhage in mice. Second, intraosseous transfusion with LEH might be very effective for even such a serious hemorrhage.

Consistent with survival rates, intraosseous transfusion with LEH significantly increased Hb concentration in the mice compared with either 5% albumin or RBCs (Fig. 6B), suggesting that LEH can effectively flow into the systemic circulation from the femur, unlike RBCs. Intraosseous transfusion with either LEH or 5% albumin increased neither RBC count nor hematocrit in the mice 1 h after transfusion, although intraosseous transfusion with RBCs gave such an increase (but slight) (Fig. 6, C and D), because the hematology analyzer cannot detect the LEH vesicles.

Serum TNF, erythropoietin, and plasma NO levels after intraosseous transfusion

Intraosseous transfusion with RBCs increased serum TNF levels in mice immediately after the transfusion (at 5 min) and kept them higher levels, in contrast to intraosseous transfusion with LEH or 5% albumin (Fig. 7A). Because intraosseous transfusion with LEH tended to increase hematocrit and RBC count beyond 48 h after the transfusion (Fig. 6, C and D), we examined the effect of LEH on the induction of erythropoietin, which stimulates RBC production in the bone marrow. Erythropoietin levels were increased after intraosseous transfusion and peaked at 12 h in all three groups. However, there was no significant difference in the erythropoietin levels among the three groups (Fig. 7B), suggesting that LEH does not affect erythropoietin-stimulated RBC production in the bone marrow. No significant decreases in the plasma NO_2^- or NO_3^- levels were observed in the mice after intraosseous transfusion with LEH relative to levels with 5% albumin or RBCs (Fig. 7C and D), suggesting that LEH does not have a potent NO scavenging effect, similar to our results for intravenous transfusion.

Resuscitation of massive hemorrhage model by intravenous transfusion with LEH or RBCs

Finally, we examined the effect of intravenous transfusion with LEH or RBCs on the mouse survival in this hemorrhage model. After the second blood withdrawal, the mice were intravenously transfused with LEH (n = 10), 5% albumin (n = 10),

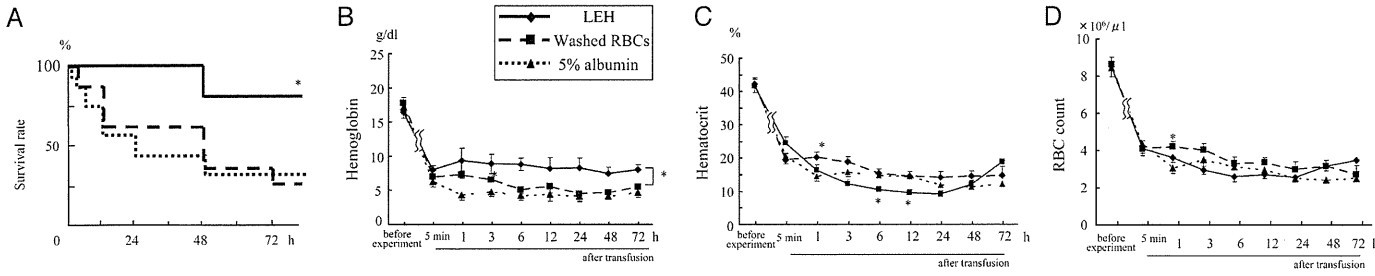

FIG. 6. **The effect of intraosseous transfusion on the survival (A), Hb level (B), hematocrit (C), and RBC count (D) in mice.** The mice had 0.8 mL of blood withdrawn followed by intraosseous infusion with 1 mL of 5% albumin. Subsequently, they had 0.3 mL of additional blood withdrawn. Thereafter, the mice were treated by intraosseous transfusion with 1 mL of either LEH, 5% albumin, or washed RBCs. Data are mean ± SE from 10 mice in each group. $*P < 0.05$ vs. the other groups.

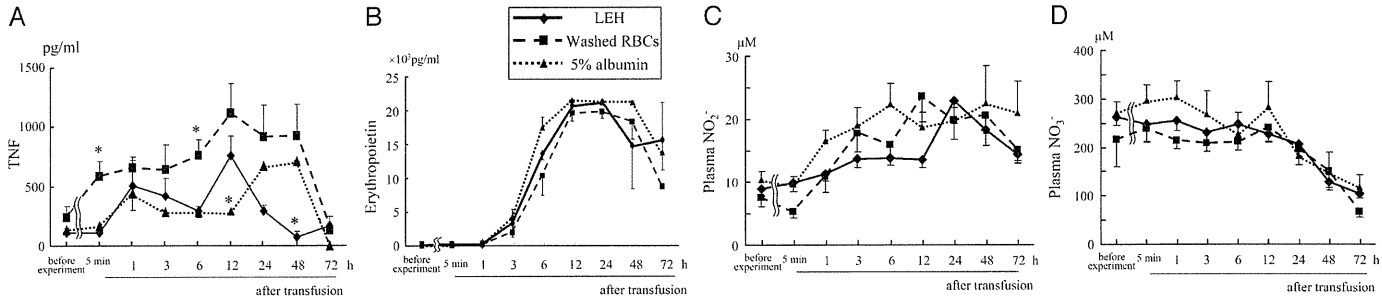

FIG. 7. **The change in serum TNF (A), erythropoietin (B), plasma NO_2^- (C), and NO_3^- (D) levels in mice after intraosseous transfusion.** The mice had blood withdrawn and intraosseous infusion as described in Figure 5. The changes in serum/plasma mediators after intraosseous transfusion with LEH, 5% albumin, or washed RBCs are shown. Data are mean ± SE from 10 mice in each group. $*P < 0.05$ vs. the other groups.

or RBCs (n = 10). As expected, intravenous transfusion with RBCs effectively increased mouse survival as well as that with LEH (Fig. 8A). Consistently, intravenous transfusion with RBCs significantly increased Hb concentration, hematocrit, and RBC count in the mice after transfusion (Fig. 8, B–D), suggesting an effective and rapid replenishment of RBC in the systemic circulation.

DISCUSSION

Intraosseous transfusion with LEH more effectively rescued mice from fatal hemorrhage without scavenging NO than did intraosseous transfusion with RBCs. The present study clearly demonstrates the advantage of LEH, relative to conventional blood transfusion, as a blood substitute in resuscitation from massive hemorrhage in prehospital environment.

Despite many physiological modifications of Hb (2), cell-free Hbs reportedly increased the risk of myocardial infarction and death in a meta-analysis of the data from the clinical trials (7). These disadvantages of cell-free Hbs are thought to derive from their vasopressor effect, resulting from NO scavenging (2, 9, 10). Thus, NO scavenging induced by cell-free Hbs must be one of the most serious and fundamental adverse effects of the resuscitation of patients with hemorrhagic shock. Cross-linkage and/or polymerization of cell-free Hbs seem to be insufficient to prevent NO scavenging, because basically they do not have a structure like a cellular membrane, which may be indispensable in preventing direct contact between Hb and NO.

It is noteworthy that the current encapsulated Hb induced neither an NO scavenging effect nor elevation of serum TNF in mice after either intravenous or intraosseous transfusion. Mice receiving intravenous or intraosseous transfusion with LEH showed no marked decrease in the plasma NO_2^- or NO_3^- levels. Although the mice transfused with RBCs also showed no decrease in NO_3^- levels, $NO2^-$ levels were promptly increased after intravenous RBC transfusion. Regarding this, it has been reported that blood pressure decreased after isovolemic exchange transfusion with RBCs, in which increased blood viscosity induced shear stress–mediated production of NO in endothelial cells, leading to vasodilatation and hypotension (18–20). We speculate that a similar mechanism may explain the increased NO production in the first RBC infusion model. This is a first report measuring the plasma NO_2^- and NO_3^- levels after HBOC transfusion and, more importantly, showing a significant protection from both NO_2^- and NO_3^- scavenging effects induced by HBOC. Our novel HBOC, namely LEH, might have a potential for rescuing hemorrhagic shock patients without NO scavenging.

The intraosseous infusion route is reported to be a viable means of blood transfusion in a nonhemorrhagic swine model (21). Crystalloid infusion via the intraosseous route with a fixed (not rapid) rate was as effective as peripheral and central intravenous accesses for reversible hemorrhagic shock (22). However, the tortuous vascular architecture in the bone marrow might cause substantial hydraulic resistance to rapid infusion with fluid. The flow volume of intraosseous infusion with RBCs was significantly smaller than for saline under both normal gravitational and 300-mmHg pressures (23). Thus, rapid transfusion with RBCs via the intraosseous route may not be effective in rescuing the host from hemorrhagic shock. Therefore, crystalloid or colloid fluid infusion via intraosseous route is usually used for hypovolemic shock. However, asanguineous fluid cannot rescue the patients from fatal severe

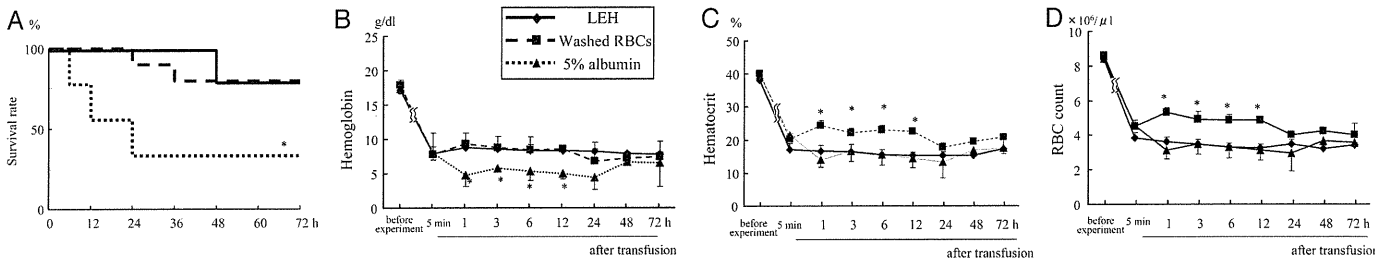

FIG. 8. **The effect of intravenous transfusion on the survival (A), Hb level (B), hematocrit (C), and RBC count (D) in mice.** The mice had 0.8 mL of blood withdrawn from the femoral vein and intraosseous infusion with 1 mL of 5% albumin. Subsequently, they had 0.3 mL of additional blood withdrawn. Thereafter, the mice were treated by intravenous transfusion with 1 mL of either LEH, 5% albumin, or washed RBCs. Data are mean ± SE from 10 mice in each group. $*P < 0.05$ vs. the other groups.

anemia resulting from massive Hb loss and tissue hypoxia (12), and administration of an oxygen carrier including LEH or RBCs is preferable for resuscitation in that situation.

Thus, we tried to establish the simple model with intraosseous infusion after blood exchange. However, this model did not succeed because approximately 90% of the animals were dropped because of anesthetic problems, unexpected cardiac arrest, or bleeding when attempting the intraosseous route. The second model tried to reproduce resuscitation in a clinical situation when another hemorrhage occurs after adequate asanguineous infusion for an initial hemorrhage. Whereas approximately 32% of the original Hb remained after blood exchange and transfusion in the first dilution model, 40% of original Hb remained in the second model, which may explain the fact that the mouse survival after intraosseous albumin infusion was better than intravenous albumin transfusion.

Intraosseous transfusion with LEH significantly increased the survival of and the Hb levels in mice above those seen with RBCs. Because the size of the LEH vesicle is about 220 nm, which is 1/30 to 1/40 the size of a natural mouse RBC, the influx of LEH from the femur to the systemic circulation might be better than RBC influx, thereby improving mouse survival. Furthermore, the biconcave shape, size, and deformability of natural RBCs might be appropriate for passing quickly through capillaries, but perhaps not through the tortuous vascular architecture in the bone marrow. The round shape, smaller size, and elastic hardness of LEH vesicles may be more suitable for the intraosseous route. Extravasation of infusions and compartment syndrome occasionally occur in intraosseous infusion and may be associated with major morbidity. When we intraosseously transfused RBC into the mice at high pressure, extravasation of RBCs was sometimes observed around the inserting site by pressure infusion. Extravasation occurred more frequently after RBC transfusion than after LEH transfusion. Interestingly, TNF levels after intraosseous RBC transfusion were higher than those after LEH or 5% albumin treatment. Because washed RBCs cannot pass through the tortuous vascular architecture in the bone marrow smoothly, activated bone marrow macrophages may phagocytose trapped RBCs and produce TNF.

As expected, intravenous transfusion with RBCs effectively rescued the mice from fatal hypohemoglobinemia, whereas intravenous transfusion with LEH eventually could not rescue more than half of the mice (although it could rescue most of them within several hours). Some investigators have pointed out similar problems, in that the effective period of cell-free Hb is not very long (24). A clinical report on a bovine-derived Hb solution (HBOC-201; Hemopure, OPK Biotech, Cambridge, Mass) in South Africa has demonstrated that some patients presented severe anemia again 24 to 36 h after the initial administration to relieve life-threatening symptoms of anemia (24). Although mice intravenously transfused with LEH showed a change in Hb levels similar to that of mice transfused with RBCs, their survival rates were quite different. Liposome-encapsulated hemoglobin may lose its function as an oxygen carrier soon after transfusion. The functional half-life of LEH has been reported as approximately 6 h in mice (25). Although the present LEH has a long circulation time achieved by modification of the liposomal surface with hydrophilic polymer, it was reported that the functional half-life (the period to a reduction by half of actual oxygen transport efficiency) seems to be shorter than natural Hb half-life because of methemoglobin generation (10, 25, 26). Methemoglobin formation might be one of the reasons why the LEH-transfused mice showed lower survival rates than did RBC-transfused mice despite similar Hb levels. However, transfusion with LEH saved mice for 6 h, although no mice were rescued by albumin transfusion. If survival is extended beyond 6 h, the possibility of the medical team rescuing the patient increases. Red blood cell transfusion after resuscitation with LEH may improve the survival of hypohemoglobinemic shock patients. In addition, the half-life of LEH in rat and monkey was about 10 and 70 h, respectively; therefore, a longer half-life of LEH could be anticipated in humans (10).

The present study indicates a need for transfusion with an oxygen carrier after conventional fluid resuscitation in situations of uncontrolled massive hemorrhage that can lead to fatal hypohemoglobinemia. In a hospital environment, intraosseous infusion is not needed except in special situations, because the medical staff can insert a central venous catheter for transfusion. In a prehospital environment such as a battlefield or in a confined space in disaster situations, however, sometimes only the intraosseous route will be available. If LEH can be administrated to patients via the intraosseous route, resuscitation using oxygen-carrying fluid can be performed under critical conditions without special training or medical expertise.

REFERENCES

1. Manning JE, Katz LM, Brownstein MR, Pearce LB, Gawryl MS, Baker CC: Bovine hemoglobin-based oxygen carrier (HBOC-201) for resuscitation of uncontrolled, exsanguinating liver injury in swine. Carolina resuscitation research group. *Shock* 13:152–159, 2000.
2. Squires JE: Artificial blood. *Science* 295:1002–1005, 2002.
3. Johnson T, Arnaud F, Dong F, Philbin N, Rice J, Asher L, Arrisueno M, Warndorf M, Gurney J, McGwin G, et al.: Bovine polymerized hemoglobin (hemoglobin-based oxygen carrier-201) resuscitation in three swine models of hemorrhagic shock with militarily relevant delayed evacuation—effects on histopathology and organ function. *Crit Care Med* 34:1464–1474, 2006.
4. Kasper SM, Walter M, Grune F, Bischoff A, Erasmi H, Buzello W: Effects of a hemoglobin-based oxygen carrier (HBOC-201) on hemodynamics and oxygen transport in patients undergoing preoperative hemodilution for elective abdominal aortic surgery. *Anesth Analg* 83:921–927, 1996.
5. Schubert A, O'Hara JF Jr, Przybelski RJ, Tetzlaff JE, Marks KE, Mascha E, Novick AC: Effect of diaspirin crosslinked hemoglobin (DCLHb HemAssist) during high blood loss surgery on selected indices of organ function. *Artif Cells Blood Substit Immobil Biotechnol* 30:259–283, 2002.
6. Kerner T, Ahlers O, Veit S, Riou B, Saunders M, Pison U: DCL-Hb for trauma patients with severe hemorrhagic shock: the European "on-scene" multicenter study. *Intensive Care Med* 29:378–385, 2003.
7. Natanson C, Kern SJ, Lurie P, Banks SM, Wolfe SM: Cell-free hemoglobin-based blood substitutes and risk of myocardial infarction and death: a meta-analysis. *JAMA* 299:2304–2312, 2008.
8. Stern S, Rice J, Philbin N, McGwin G, Arnaud F, Johnson T, Flournoy WS, Ahlers S, Pearce LB, McCarron R, et al.: Resuscitation with the hemoglobin-based oxygen carrier, HBOC-201, in a swine model of severe uncontrolled hemorrhage and traumatic brain injury. *Shock* 31:64–79, 2009.
9. Ogata Y, Goto H, Kimura T, Fukui H: Development of neo red cells (NRC) with the enzymatic reduction system of methemoglobin. *Artif Cells Blood Substit Immobil Biotechnol* 25:417–427, 1997.
10. Kaneda S, Ishizuka T, Goto H, Kimura T, Inaba K, Kasukawa H: Liposome-encapsulated hemoglobin, trm-645: current status of the development and important issues for clinical application. *Artif Organs* 33:146–152, 2009.
11. Sakai H, Sou K, Horinouchi H, Kobayashi K, Tsuchida E: Haemoglobin-vesicles as artificial oxygen carriers: present situation and future visions. *J Intern Med* 263:4–15, 2008.

12. Nogami Y, Kinoshita M, Takase B, Ogata Y, Saitoh D, Kikuchi M, Ishihara M, Maehara T: Liposome-encapsulated hemoglobin transfusion rescues rats undergoing progressive hemodilution from lethal organ hypoxia without scavenging nitric oxide. *Ann Surg* 248:310–319, 2008.
13. Drinker C, Drinker K, Lund C: The circulation in the mammalian bone marrow. *Am J Physiol* 62:1–92, 1922.
14. Henning N: Intrasternal injections and transfusion. *JAMA* 128:240, 1945.
15. Dubick MA, Holcomb JB: A review of intraosseous vascular access: current status and military application. *Mil Med* 165:552–559, 2000.
16. Sakai H, Masada Y, Horinouchi H, Yamamoto M, Ikeda E, Takeoka S, Kobayashi K, Tsuchida E: Hemoglobin-vesicles suspended in recombinant human serum albumin for resuscitation from hemorrhagic shock in anesthetized rats. *Crit Care Med* 32:539–545, 2004.
17. Tait AR, Larson LO: Resuscitation fluids for the treatment of hemorrhagic shock in dogs: effects on myocardial blood flow and oxygen transport. *Crit Care Med* 19:1561–1565, 1991.
18. Martini J, Carpentier B, Negrete AC, Frangos JA, Intaglietta M: Paradoxical hypotension following increased hematocrit and blood viscosity. *Am J Physiol Heart Circ Physiol* 289:H2136–H2143, 2005.
19. Uematsu M, Ohara Y, Navas JP, Nishida K, Murphy TJ, Alexander RW, Nerem RM, Harrison DG: Regulation of endothelial cell nitric oxide synthase mRNA expression by shear stress. *Am J Physiol* 269:C1371–C1378, 1995.
20. Dimmeler S, Zeiher AM: Endothelial cell apoptosis in angiogenesis and vessel regression. *Circ Res* 87:434–439, 2000.
21. Bell MC, Olshaker JS, Brown CK, McNamee GA Jr, Fauver GM: Intraosseous transfusion in an anesthetized swine model using ^{51}Cr-labeled autologous red blood cells. *J Trauma* 31:1487–1489, 1991.
22. Neufeld JD, Marx JA, Moore EE, Light AI: Comparison of intraosseous, central, and peripheral routes of crystalloid infusion for resuscitation of hemorrhagic shock in a swine model. *J Trauma* 34:422–428, 1993.
23. Schoffstall JM, Spivey WH, Davidheiser S, Lathers CM: Intraosseous crystalloid and blood infusion in a swine model. *J Trauma* 29:384–387, 1989.
24. Levien LJ. South Africa: clinical experience with Hemopure. *ISBT Sci Ser* 1:167–173, 2006.
25. Tsutsui Y, Kimura T, Ishizuka T, Oomori S, Shizawa T, Goto H, Ogata Y, Kaneda S: Duration of efficacy of NRC (neo red cell) in a rat hemodilution model [in Japanese]. *Artif Blood* 10:36–41, 2002.
26. Tsutsui Y, Ishizuka T, Goto H, Kimura T, Ogata Y, Kaneda S: Duration of efficacy of NRC (neo red cell) administered in divided doses [in Japanese]. *Artif Blood* 11:200–204, 2003.

0090-9556/11/3903-484–489$20.00
DRUG METABOLISM AND DISPOSITION
Copyright © 2011 by The American Society for Pharmacology and Experimental Therapeutics
DMD 39:484–489, 2011

Vol. 39, No. 3
36913/3666427
Printed in U.S.A.

Repeated Injection of High Doses of Hemoglobin-Encapsulated Liposomes (Hemoglobin Vesicles) Induces Accelerated Blood Clearance in a Hemorrhagic Shock Rat Model

Kazuaki Taguchi, Yasunori Iwao, Hiroshi Watanabe, Daisuke Kadowaki, Hiromi Sakai, Koichi Kobayashi, Hirohisa Horinouchi, Toru Maruyama, and Masaki Otagiri

Department of Biopharmaceutics (K.T., Y.I., H.W., D.K., T.M., M.O.), Center for Clinical Pharmaceutical Sciences (H.W., D.K., T.M.), Graduate School of Pharmaceutical Sciences, Kumamoto University, Kumamoto, Japan; Faculty of Pharmaceutical Sciences, Sojo University, Kumamoto, Japan (M.O.); Research Institute for Science and Engineering, Waseda University, Tokyo, Japan (H.S.); and Department of Surgery, School of Medicine, Keio University, Tokyo, Japan (K.K., H.H.)

Received October 24, 2010; accepted December 1, 2010

ABSTRACT:

The hemoglobin vesicle (HbV) is an artificial oxygen carrier in which a concentrated hemoglobin solution is encapsulated in a liposome. To apply liposome preparations in clinics, it is important to consider the accelerated blood clearance phenomenon (ABC phenomenon), which involves a loss in the long-circulation half-life after being administered repeatedly to the same animals. The objective of this study was to determine whether the ABC phenomenon is induced by repeated injection of HbV under conditions of hemorrhagic shock. We created a rat model of hemorrhagic shock and performed a pharmacokinetic study using ^{125}I-HbV, in which the Hb inside of HbV was labeled with ^{125}I. At 4 and 7 days after resuscitation from hemorrhagic shock by nonlabeled HbV (1400 mg Hb/kg), the second dose of ^{125}I-HbV (1400 mg Hb/kg) was rapidly cleared from the circulation compared with normal rats. Of interest, IgM against HbV was produced at 4 days after the first injection of HbV, but decreased at 7 days. In addition, phagocyte activity was increased at both 4 and 7 days after the first injection of HbV. These results suggest that repeated injections of HbV at a dose of 1400 mg Hb/kg induce the ABC phenomenon under conditions of hemorrhagic shock, which is strongly related to both the production of anti-HbV IgM and enhanced phagocyte activity. We thus conclude that it might be necessary to considerer the ABC phenomenon in the dose regimen of HbV treatment in clinical settings.

Introduction

Hemoglobin-based artificial oxygen carriers (HBOCs), which include cross-linked (Chen et al., 2009), polymerized (Jahr et al., 2008), and polymer-conjugated Hb (Smani, 2008), have been developed to overcome problems associated with blood transfusion, such as cross-matching, blood-bone infections (human immunodeficiency virus and hepatitis virus), and the shortage of donated blood. Several of these HBOCs are currently in the final stages of clinical evaluation. However, Natanson et al. (2008) recently performed a meta-analysis based on data from randomized controlled trials of five different acellular-type HBOCs and concluded that acellular-type HBOCs are associated with a significantly increased risk of death and myocardial infarction. This risk would be induced by the scavenging of nitric oxide (NO) by cell-free Hb, because it was reported that a reduction in NO levels in myocardial lesions is an important factor in inducing histological damage in cases of myocardial lesions (Burhop et al., 2004).

This work was supported in part by the Ministry of Health, Labor and Welfare of Japan ([Health Sciences Research Grants].

Article, publication date, and citation information can be found at http://dmd.aspetjournals.org.

doi:10.1124/dmd.110.036913.

The hemoglobin vesicle (HbV) is an artificial oxygen carrier with a cellular structure (liposome structure) similar to that of red blood cells (RBCs): highly concentrated Hb encapsulated in a phospholipid bilayer membrane with polyethylene glycol (PEG). Because this membrane reduces interactions between Hb and NO, adverse effects, such as hypertension and histological damage in myocardial lesions, are not induced, as are found for acellular-type HBOCs (Sakai et al., 2000, 2004a). In addition, there are some distinct advantages associated with the membrane structure of HbV as follows; the oxygen affinity (P_{50}) of HbV can be easily regulated by manipulating the content of an allosteric effector such as pyridoxal 5′-phosphate (Sakai and Tsuchida, 2007), an enhanced lifetime in the blood circulation compared with other types of HBOCs (Sou et al., 2005; Taguchi et al., 2009c), guarantees long-term storage for periods of more than 2 years at room temperature (Tsuchida et al., 2009). Moreover, HbV possesses oxygen transport characteristics that are comparable to those of RBCs. In fact, the pharmacological effects of HbV have been reported to be equivalent to that of RBCs, when injected into hemorrhagic shock animals (Sakai et al., 2004b, 2009). Therefore, HbV has attracted considerable attention as a potential candidate for use as an artificial oxygen carrier and has considerable promise for use in clinical settings.

ABBREVIATIONS: HBOC, hemoglobin-based artificial oxygen carrier; NO, nitric oxide; HbV, hemoglobin vesicle; RBC, red blood cell; PEG, polyethylene glycol; ABC phenomenon, accelerated blood clearance phenomenon; SD, Sprague-Dawley; HS, hemorrhagic shock; MZ, marginal zone.

It was reported that PEGylated liposomes showed some unexpected pharmacokinetic properties, the so-called accelerated blood clearance phenomenon (ABC phenomenon), in which the long-circulation half-life is lost after liposomes are administered twice to the same animals (Laverman et al., 2001; Ishida and Kiwada, 2008). Ishida et al. (2006a) proposed a mechanism for the ABC phenomenon as follows. IgM, produced in the spleen by the first injection of PEGylated liposomes, selectively binds to the second injected PEGylated liposomes and subsequent complement activation by IgM results in accelerated clearance and enhanced hepatic uptake of the second injected dose of PEGylated liposomes. In the case of HbV, there have been several explanations for the induction of the ABC phenomenon as follows: 1) HbV has a liposome structure that contains PEG; 2) our previous study, using normal mice, showed that the ABC phenomenon was not induced, but anti-HbV IgM was produced 7 days after the injection of HbV at a dose of 1400 mg Hb/kg (Taguchi et al., 2009c); and 3) the pharmacokinetic properties of HbV are altered under the various pathological conditions (Taguchi et al., 2009a, 2010). Therefore, it is possible that the pharmacokinetics of HbV become altered by repeated administration in various pathological conditions. In a clinical setting, HbV would be used to treat a massive hemorrhage, and repeated administrations would be required. If the pharmacokinetics of HbV were altered as the result of repeated injections, then the pharmacological action of HbV would probably be influenced. Therefore, it becomes necessary to clarify the pharmacokinetics associated with the repeated injection of HbV under conditions of massive hemorrhage.

The objective of the present study was to investigate whether the ABC phenomenon is induced by repeated injection of HbV under conditions of massive hemorrhage. To accomplish this, we examined changes in the pharmacokinetics of HbV, using ^{125}I-HbV [the internal Hb of HbV was directly labeled with iodine (^{125}I)], during repeated administration using a rat model of hemorrhagic shock. In addition, we further studied the mechanism of the induction of the ABC phenomenon under our experimental conditions.

Materials and Methods

Preparation of HbV. HbV was prepared under sterile conditions as reported previously (Sakai et al., 1997). In brief, an Hb solution was purified from outdated donated blood provided by the Japanese Red Cross Society (Tokyo, Japan). The encapsulated Hb (38 g/dl) contained 14.7 mM pyridoxal 5′-phosphate (Sigma-Aldrich, St. Louis, MO) as an allosteric effector to maintain the P_{50} to 25–28 Torr. The lipid bilayer was a mixture of 1,2-dipalmitoyl-*sn*-glycero-3-phosphatidylcholine, cholesterol, and 1,5-bis-*O*-hexadecyl-*N*-succinyl-L-glutamate (Nippon Fine Chemical Co. Ltd., Osaka, Japan) at a molar ratio of 5:5:1, and 1,2-distearoyl-*sn*-glycero-3-phosphatidylethanolamine-*N*-PEG (NOF Corp., Tokyo, Japan) (0.3 mol %). The size of the HbV particles was controlled at approximately 250 nm by the extrusion method used. The HbV was suspended in a physiological salt solution at [Hb] 10 g/dl, filter-sterilized (pore size 450 nm; Dismic, Toyo-Roshi, Tokyo, Japan) and bubbled with N_2 for storage. The lipopolysaccharide content was <0.1 endotoxin unit/ml.

Before all experiments, HbV was mixed with recombinant human serum albumin (Nipro Corp., Osaka, Japan) to adjust the albumin concentration of the suspension medium to 5 g/dl. Under these conditions, the colloid osmotic pressure of the suspension can be kept constant at approximately 20 mm Hg (Sakai et al., 2004b).

Preparation of Hemorrhagic Shock Model Rats. All animal experiments were performed according to the guidelines, principles, and procedures of Kumamoto University for the care and use of laboratory animals. SD rats were maintained in a temperature-controlled room with a 12-h dark/light cycle and ad libitum access to food and water. Hemorrhagic shock model rats were prepared as described in a previous report (Taguchi et al., 2009a). Hemorrhagic shock was induced by removal of 40% of the total blood volume (22.4 ml/kg). The systemic blood volume was estimated to be 56 ml/kg (Sakai et al., 2004b). After removal of the blood, the hemorrhagic shock rats were resuscitated by an infusion of isovolemic HbV (1400 mg Hb/kg, 22.4 ml/kg). After resuscitation, all rats were housed in a temperature-controlled room with a 12-h dark/light cycle with ad libitum access to food and water.

Quantitative Determination of Anti-HbV IgG and IgM. Five SD rats with hemorrhagic shock were resuscitated with isovolemic HbV (1400 mg Hb/kg, 22.4 ml/kg). Every day after injection, blood was collected from the tail vein under ether anesthesia. Plasma was collected after centrifugation (3000*g*, 5 min), and the supernatant was subsequently ultracentrifuged to remove intact HbV (50,000*g*, 30 min) (Sakai et al., 2003). The supernatant was collected as the plasma sample and was stored at −80°C until used. The IgG and IgM against HbV were detected as described in a previous report (Taguchi et al., 2009c).

Pharmacokinetic Experiments. ^{125}I-HbV was prepared as described in a previous report (Taguchi et al., 2009b). In short, ^{125}I-HbV was prepared by incubation of HbV with Na^{125}I (PerkinElmer Life and Analytical Sciences, Waltham, NA) in an Iodogen (1,3,4,6-tetrachoro-3*a*,6*a*-diphenylglycoluril) tube for 30 min at room temperature. ^{125}I-HbV was then isolated from free ^{125}I by passage through a PD-10 column (GE Healthcare, Uppsala, Sweden). More than 97% of the total iodine was bound to the internal Hb in HbV. All suspensions were mixed with recombinant human serum albumin (5 g/dl).

All rats were given water containing 5 mM sodium iodide for the duration of the experiment to avoid specific accumulation in the glandula thyreoidea. Ten SD rats were induced with hemorrhagic shock and resuscitated with HbV, and the pharmacokinetic study was performed at 4 days (n = 5) or 7 days (n = 5) after resuscitation. Normal rats (n = 5) were also used as controls. All rats were anesthetized with pentobarbital, and polyethylene catheters were inserted into the left femoral vein. After infusion of ^{125}I-HbV (1400 mg Hb/kg), blood samples were collected at multiple time points after the ^{125}I-HbV injection (3 min, 10 min, 30 min, 1 h, 6 h, 12 h, and 24 h) and the plasma was separated by centrifugation (3000*g*, 5 min). Degraded HbV and free ^{125}I were removed from plasma by centrifugation in 1% bovine serum albumin and 40% trichloroacetic acid. After collection of the final blood samples (24 h), the rats were euthanized, and the organs were excised (kidney, liver, spleen, lung, and heart), rinsed with saline, and weighed. The levels of ^{125}I in the plasma and excised organs were determined using a gamma counter (ARC-5000; Aloka, Tokyo, Japan).

Determination of Total Blood Volume. Total blood volume was determined using the Evans blue dilution technique as described previously, with minor modifications (Kuebler et al., 2004). In brief, 4 or 7 days after resuscitation, the rats received an intravenous bolus of 1 mg of Evans blue dye in 1 ml of normal saline. At 2 min after injection, blood samples (1 ml) were collected. The samples were centrifuged, and the absorbance of each sample was measured at 620 and 750 nm. The concentration of Evans blue was determined using a standard curve of Evans blue in excess plasma in correlation to the extinction at 620 nm corrected for turbidity at 750 nm. Total blood volume was calculated using the following formula: total blood volume = total plasma volume/(100% − hematocrit (percent) × (0.01) (Clavijo-Alvarez et al., 2005).

Measurements of Phagocyte Activity. Phagocyte activity was determined by the carbon clearance method, as described in a previous report (Sakai et al., 2001; Taguchi et al., 2010). Ten SD rats were induced with hemorrhagic shock and resuscitated with HbV, and carbon clearance was determined 4 days (n = 5) or 7 days (n = 5) after resuscitation. Normal healthy rats without HbV injection (n = 5) were also used as controls. In a typical experiment, rats were anesthetized with pentobarbital. Polyethylene catheters (PE-50 tubing) containing saline and heparin were then introduced into the left femoral vein for the infusion of a carbon particle solution and for blood collection. The carbon particle solution (Fount India Ink; Pelikan, Hannover, Germany) was infused at 10 ml/kg within 1 min. At 4, 10, 20, 30, 45, and 60 min later, approximately 100 μl of blood was then withdrawn, and precisely a 50-μl aliquot was diluted with 5 ml of a 0.1% sodium bicarbonate solution. The absorption was measured at 675 nm by means of a spectrophotometer (U-2900; Hitachi, Tokyo, Japan). The phagocyte index (K) was calculated using the equation $K = 1/(t_2 - t_1) \times \ln(C_1/C_2)$, where C_1 and C_2 are the concentrations (absorbance) at time t_1 and t_2 (min), respectively.

Measurement of Carbon Activity (CH50). Ten SD rats were induced with hemorrhagic shock and resuscitated with HbV, and blood samples were col-

lected at 4 or 7 days after resuscitation. The blood was centrifuged (3000*g*, 5 min) to obtain plasma for analysis. All plasma samples were stored at −80°C before analysis by a commercial clinical testing laboratory (SRL, Tokyo, Japan). The CH50 was detected by the method of Mayer (1961).

Data Analysis. Data are shown as the mean ± S.D. for the indicated number of animals. Significant differences among each group were determined using the two-tail unpaired Student's *t* test. Pharmacokinetic analyses after HbV administration proceeded on the basis of a two-compartment model. Pharmacokinetic parameters were calculated by fitting using MULTI, a normal least-squares program (Yamaoka et al., 1981). A probability value of $p < 0.05$ was considered to indicate statistical significance.

Results

Production of Anti-HbV IgG and IgM. In a previous study, it was reported that anti-liposome IgM, produced by the preinjection of PEGylated liposomes, is strongly involved in the induction of the ABC phenomenon (Ishida et al., 2006b). Therefore, we examined the issue of whether anti-HbV IgG and IgM are produced by an initial injection of HbV at a dose appropriate for clinical use (1400 mg Hb/kg) in the rat model of hemorrhagic shock. As shown in Fig. 1, the levels of anti-HbV IgG were negligibly increased after the injection of HbV. In contrast, anti-HbV IgM was elicited starting at 3 days after resuscitation by HbV. The highest value was found at 4 days and gradually decreased until 7 days after the injection of HbV. These results suggest that repeated injection of HbV might induce the ABC phenomenon, even under conditions of hemorrhagic shock. The following experiments were performed at the time points of 4 days ($HS_{4\ day}$) and 7 days ($HS_{7\ day}$) after resuscitation by HbV.

Pharmacokinetic Study. The fate of the ^{125}I-HbV administered to normal, $HS_{4\ day}$ and $HS_{7\ day}$ rats was evaluated by determining residual trichloroacetic acid-precipitable radioactivity in the plasma. Figure 2A shows the time course for the plasma concentration of ^{125}I-HbV in normal, $HS_{4\ day}$, and $HS_{7\ day}$ rats, and Table 1 lists the pharmacokinetic parameters for these groups. Plasma retention in the $HS_{4\ day}$ and $HS_{7\ day}$ rats decreased rapidly compared with that in normal rats, and the plasma clearance of ^{125}I-HbV in the $HS_{4\ day}$ and $HS_{7\ day}$ rats was 1.7- and 1.9-fold increased compared with that in normal rats (Table 1). Accompanied by a decrease in clearance, the area under the time-concentration curve was also significantly decreased by half, whereas the elimination-phase half-life of ^{125}I-HbV was also significantly deceased in the hemorrhagic shock model rats compared with normal rats. The pharmacokinetic parameters were not significantly different between the $HS_{4\ day}$ and $HS_{7\ day}$ rats.

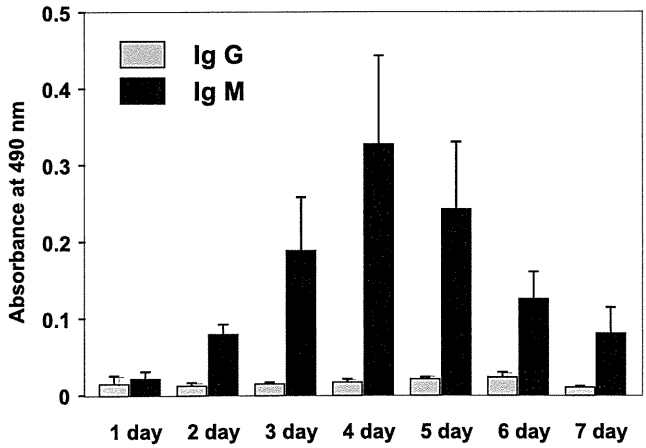

FIG. 1. The production of anti-HbV IgG and IgM after resuscitation by HbV in a rat model of hemorrhagic shock. Hemorrhagic shock was induced in SD rats with resuscitation by HbV at a dose of 1400 mg Hb/kg. After resuscitation, blood was collected from the tail vein, and plasma was obtained. Anti-HbV IgG and IgM were detected with an enzyme-linked immunosorbent assay. Each bar represents the mean ± S.D. ($n = 5$).

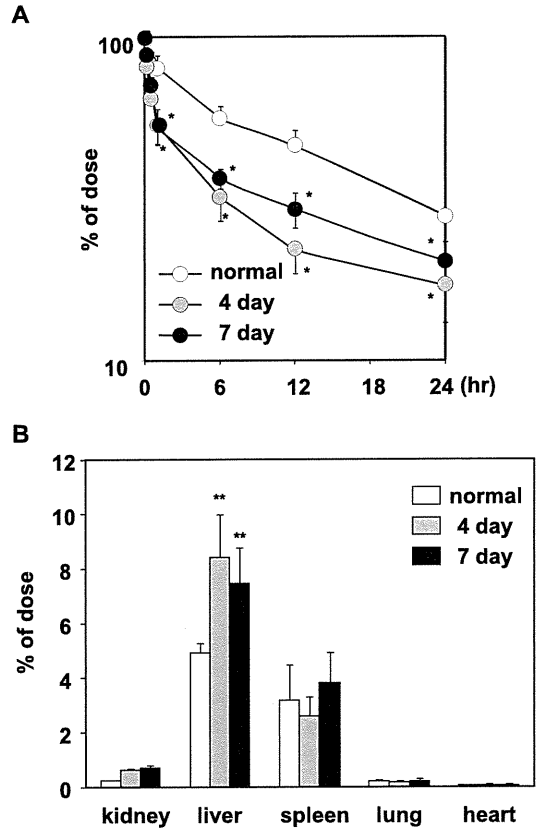

FIG. 2. A, plasma concentration curve of ^{125}I-HbV after administration to normal (○), $HS_{4\ day}$ (◎), and $HS_{7\ day}$ (●) rats at a dose of 1400 mg Hb/kg. B, tissue distributions of ^{125}I-HbV at 24 h after administration to normal (□), $HS_{4\ day}$ (▨), and $HS_{7\ day}$ (■) rats at a dose of 1400 mg Hb/kg. All rats received ^{125}I-HbV at a dose of 1400 mg Hb/kg; blood samples were collected at multiple time points (3 min, 10 min, 30 min, 1 h, 6 h, 12 h, and 24 h), and plasma samples were obtained. After collection of the final blood sample, each organ was collected at 24 h after injection. Each point represents the mean ± S.D. ($n = 5$). **, $p < 0.01$ versus normal rats.

Figure 2B shows the tissue distribution of ^{125}I-HbV (percentage of injected dose) at 24 h after ^{125}I-HbV administration. Similar to normal rats, in the $HS_{4\ day}$ and $HS_{7\ day}$ rats ^{125}I-HbV was mainly distributed in the liver and spleen. However, the amount of ^{125}I-HbV distribution in the liver was significantly increased in the $HS_{4\ day}$ and $HS_{7\ day}$ rats compared with that in normal rats, whereas that in the spleen was not significantly different among the three groups. These data indicate that the ABC phenomenon is induced in $HS_{4\ day}$ and

TABLE 1

Pharmacokinetic parameters for HbV after injections of ^{125}I-HbV in normal and hemorrhagic shock model rats

All rats received an injection of ^{125}I-HbV (1400 mg Hb/kg) containing 5% recombinant human serum albumin. At each time after the ^{125}I-HbV injection, blood was collected from the tail vein, and plasma was obtained. Each parameter was calculated by MULTI using the two-compartment model. The values are mean S.D. ($n = 5$).

	Normal	4 day	7 day
$t_{1/2\alpha}$ (h)	5.3 ± 3.9	0.53 ± 0.07*	0.47 ± 0.22*
$t_{1/2\beta}$ (h)	30.6 ± 4.0	22.3 ± 3.5*	22.0 ± 3.2*
Ke ($\times 10^3$ min^{-1})	0.70 ± 0.06	1.40 ± 0.38*	1.25 ± 0.18*
AUC (h % of dose/ml)	210.3 ± 22.9	115.9 ± 24.1*	129.4 ± 12.1*
CL (ml/h)	0.47 ± 0.04	0.90 ± 0.21*	0.78 ± 0.07*

$t_{1/2\alpha}$, the distribution-phase half-life; $t_{1/2\beta}$, the elimination-phase half-life; AUC, area under the concentration-time curve; CL, clearance.

* $p < 0.01$ versus normal.

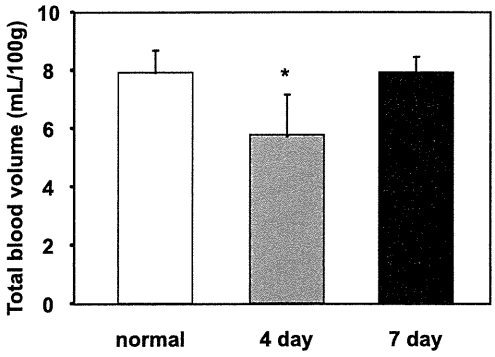

FIG. 3. Measurement of total blood volume in normal (□), $HS_{4\ day}$ (▨), and $HS_{7\ day}$ (■) rats. All rats received an intravenous bolus of 1 mg of Evans blue dye in 1 ml of NaCl. After 2 min of distribution time, blood samples (1 ml) were taken; the samples were centrifuged and the absorbance of the samples was measured at 620 and 750 nm. Total blood volume was calculated using the following formula: total blood volume = total plasma volume/(100% − hematocrit (%) × (0.01). Each bar represents the mean ± S.D. ($n = 5$). *, $p < 0.05$ versus normal rats.

$HS_{7\ day}$ rats, and this would be accompanied by an increased distribution in the liver.

Measurement of Total Blood Volume. It was previously observed that the retention of HbV in the circulation was decreased when the systemic blood volume decreased (Taguchi et al., 2009a). Therefore, we measured the total blood volume in normal, $HS_{4\ day}$, and $HS_{7\ day}$ rats using the Evans blue dilution technique. As shown in Fig. 3, the total blood volume in the $HS_{4\ day}$ rats was significantly changed, but this change was not remarkable compared with the massive bleeding. These data indicate that the shorter retention in the circulation in the $HS_{4\ day}$ and $HS_{7\ day}$ rats was not due to a decreased systemic blood volume and that other factors are strongly involved in this phenomenon.

Complement Activity. It is well known that the ABC phenomenon is induced by the selective binding of anti-liposome IgM to the second injected PEGylated liposomes, and subsequent complement activation by IgM results in accelerated clearance and enhanced hepatic uptake of the second injected PEGylated liposomes (Ishida and Kiwada, 2008). Therefore, we also measured the complement activity (CH50) in normal healthy, $HS_{4\ day}$, and $HS_{7\ day}$ rats.

As a result, the CH50 in $HS_{4\ day}$ and $HS_{7\ day}$ rats was significantly decreased compared with that in normal rats [38.0 ± 7.9/ml, 17.1 ± 9.4/ml ($p < 0.01$), and 30.8 ± 11.0/ml ($p < 0.05$), for normal, $HS_{4\ day}$, and $HS_{7\ day}$ rats, respectively]. However, the degree of the difference between normal healthy and $HS_{7\ day}$ rats was remarkably less than that observed between normal healthy and $HS_{4\ day}$ rats. These results suggest that the induction of the ABC phenomenon in $HS_{4\ day}$ rats is caused by an increase in complement activation, whereas that in $HS_{7\ day}$ can be mainly attributed to other mechanisms.

Phagocyte Activity. Phagocyte activity is strongly related to hepatic uptake and the induction of the ABC phenomenon. Therefore, we hypothesized that phagocyte activity, especially in Kupffer cells, would be altered after resuscitation by HbV injection. To examine the possible changes in phagocyte activity, we estimated the carbon clearance, which is an indication of phagocyte activity in Kupffer cells (Kupffer cells phagocytes were more than 90% of the injected carbon particles).

As shown in the Fig. 4, the phagocyte activity in $HS_{4\ day}$ rats was approximately 1.5 times higher than that in normal healthy rats. Of interest, compared with normal healthy rats, phagocyte activity was doubled in the $HS_{7\ day}$ rats. These data indicate that phagocyte activity is increased after resuscitation by HbV in the rat model of hemorrhagic shock, and the enhanced phagocyte activity might affect the induction of the ABC phenomenon.

Discussion

The induction of the ABC phenomenon can be described for a time frame involving two phases: the induction phase, after the first injection, during which the immune system is primed (reflected in the production of anti-liposome IgM), and the effectuation phase, after the second injection, during which PEG liposomes are rapidly cleared from the bloodstream (reflected in the enhanced uptake by Kupffer cells) (Laverman et al., 2001). In the present study, repeated injections of HbV to a hemorrhagic shock rat model at a dose of 1400 mg Hb/kg seems to induce the ABC phenomenon, and this phenomenon appears to be strongly related to changes that occur during the induction phase, in which the anti-HbV IgM was increased, and the effectuation phase, in which the phagocyte activity in Kupffer cells becomes enhanced by the initially injected HbV.

In the case of the induction phase, it is important to consider the interaction of liposomes with the marginal zone (MZ) in the spleen, which is defined as the junction of the red pulp and white pulp, and contains macrophages, dendritic cells, and B cells (MZ B cells). It was recently proposed that the induction mechanism of anti-liposome IgM involves the localization of liposomes in a certain functional splenic compartment after intravenous injection might be essential and that interaction with immune cells, B cells (but not T cells), in the spleen is critical in the development of this immune response against liposomes (Ishida et al., 2006b, 2007). In addition, it was reported that splenic MZ B cells produce large amounts of IgM within 3 to 4 days after stimulation (Martin et al., 2001). In this study, the production of anti-HbV IgM, but not that of anti-HbV IgG, started from 3 days after the first injection of HbV for resuscitation from hemorrhagic shock (Fig. 1) as well as previous studies using normal rats. Therefore, in the case of HbV injection for a hemorrhagic shock rat model, anti-HbV IgM would be produced via an interaction with splenic MZ B cells, similar to other liposome preparations.

However, it was previously reported that the production of anti-liposome IgM is suppressed with an increase in the first injected dose, and consequently the induction of the ABC phenomenon was inhibited (Wang et al., 2007). Although the dosage amount of HbV in this study was more than 100 times higher than that of other liposome preparations, anti-HbV IgM production was also induced (Fig. 1). This difference can be attributed to differences in physicochemical properties and structure, such as particle size or charge on the surface, between HbV and liposomes used in previous studies. In fact, Demoy et al. (1999) reported that particles with different surface charges and diameters showed differences in uptake by the spleen as well as

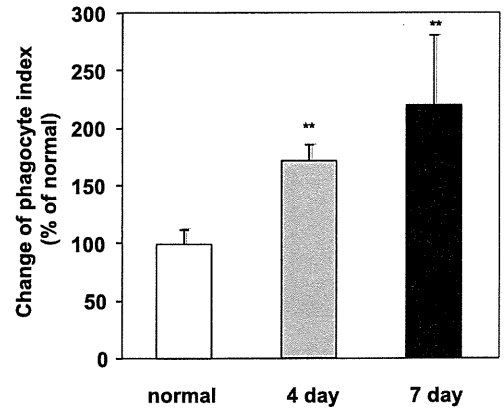

FIG. 4. The phagocyte index (K) in normal (□), $HS_{4\ day}$ (▨), and $HS_{7\ day}$ (■) rats. Carbon clearance was estimated, and K was calculated from the clearance of carbon particles. Each bar represents the mean ± S.D. ($n = 5$). **, $p < 0.01$ versus normal rats.

localization in the spleen compartment. The diameter and zeta potential of the HbV particles were −18.7 mV and approximately 250 nm, respectively (Tsuchida et al., 2009), whereas the liposomes used in previous reports were −1.5 mV and approximately 100 nm, respectively (Ishida et al., 2006b). In addition, senescent RBCs are finally captured and degraded by macrophages in splenic MZ cells. Because, unlike other liposomes, the structure of an HbV particle is similar to those of RBCs, it is possible that HbV would interact with MZ cells, which might play an important role in the production of anti-HbV IgM.

The effectuation phase is reflected in an enhanced uptake by the mononuclear phagocyte system, especially Kupffer cells. The carbon clearance measurements showed that systematic phagocyte activity increased by approximately 1.5- and 2-fold at 4 and 7 days, respectively, after the HbV infusion (Fig. 4). A similar phenomenon was recently reported for HbV using normal rats; systematic phagocyte activity began to increase 3 days after an HbV infusion at a dose of 2000 mg Hb/kg, and this value reached a maximum 7 days after HbV infusion (Sakai et al., 2001). From the present limited data, we cannot, with certainty, clarify the mechanism responsible for the enhancement in phagocyte activity that accompanies the administration of HbV. Previous studies reported that the composition of the lipid membrane and the size of the nanoparticles affected the phagocyte activity of mononuclear phagocyte system several days after their infusion in mice (Allen et al., 1984; Fernández-Urrusuno et al., 1996). Therefore, the physicochemical properties of HbV such as the components of the lipid membrane and particle size might also contribute to the induction of phagocyte activity.

Moreover, the possibility that the pathological conditions in our study might have had an effect on the changes in phagocyte activity cannot be excluded. It was previous reported that phagocyte activity, especially Kupffer cells, increased after hemorrhagic shock (Hunt et al., 2001). Under this condition, Kupffer cells exposed to hypoxia and reoxygenation were activated and generated oxidative stress and cytokines, which subsequently further stimulated the Kupffer cells (Rymsa et al., 1991). Moreover, primed and activated Kupffer cells are also stimulated by activated complement factors. Jaeschke et al. (1993) demonstrated that Kupffer cells were activated by complement under conditions of hepatic ischemia reperfusion. In fact, in the previous studies of HbV administration into healthy rats, the complement activation was minimal (Abe et al., 2007; Sou and Tsuchida, 2008), and the profile was significantly different from that observed in the present study. Because it is well known that ischemia reperfusion is induced even in the course of hemorrhagic shock and resuscitation, these factors might also be important for the incremental increase in phagocyte activity in this study.

To our knowledge, this is the first examination of the ABC phenomenon using a liposome preparation in conjunction with a model of a pathological condition and provides evidence for the induction of the ABC phenomenon under conditions of hemorrhagic shock. However, our model has several limitations with respect to extrapolating it for use in a human clinical setting. The present studies involved the use of a 40% bleeding model, which was indicated for an RBC transfusion in clinics. Because a massive hemorrhage frequently occurs as the result of a traffic accident or a related injury, it would be expected that the amount of bleeding would exceed 40% of total systemic blood volume. Goins et al. (1995) reported that the circulation kinetics and organ distribution vary among different hypovolemic exchange transfusions with liposome-encapsulated hemoglobin. In addition, the pathological conditions involved, such as blood flow and immunoresponses, can change with the amount of bleeding. Therefore, the induction of anti-HbV IgM and phagocyte activity might be affected by different amounts of bleeding. Similar experiments using a more severe bleeding model should be one of the subjects of future investigation. Moreover, the induction of the ABC phenomenon has been observed in mice, rats, and the rhesus monkey (Dams et al., 2000; Ishida et al., 2003). The injected time interval for the induction of the ABC phenomenon was not consistent with each animal. This implies that extrapolating the present findings obtained using a rat model to human for clinical applications is not an easy task. Therefore, it will be necessary to examine the characteristics of the ABC phenomenon among different animal models of hemorrhagic shock in determining a clinical dosage regimen for HbV.

In conclusion, the present study clearly demonstrates that repeated injections of HbV at a dose of 1400 mg Hb/kg induce the ABC phenomenon in rats under conditions of hemorrhagic shock and that this is associated with the production of anti-HbV IgM and an enhancement in phagocyte activity. These results suggest that, in a clinical situation, the repeated use of HbV in patients with a massive hemorrhage would be expected to induce the ABC phenomenon. Therefore, it may be necessary to considerer the ABC phenomenon in an administration schedule or regimen when HbV is used as a RBC substitute.

Acknowledgments

We thank Emeritus Professor Eishun Tsuchida for his support regarding our research.

Authorship Contributions

Participated in research design: Taguchi, Iwao, Watanabe, Kadowaki, and Otagiri.

Conducted experiments: Taguchi.

Contributed new reagents or analytic tools: Sakai, Kobayashi, Horinouchi, and Maruyama.

Performed data analysis: Taguchi and Kadowaki.

Wrote or contributed to the writing of the manuscript: Taguchi, Watanabe, Sakai, Maruyama, and Otagiri.

References

Abe H, Azuma H, Yamaguchi M, Fujihara M, Ikeda H, Sakai H, Takeoka S, and Tsuchida E (2007) Effects of hemoglobin vesicles, a liposomal artificial oxygen carrier, on hematological responses, complement and anaphylactic reactions in rats. *Artif Cells Blood Substit Immobil Biotechnol* **35:**157–172.

Allen TM, Murray L, MacKeigan S, and Shah M (1984) Chronic liposome administration in mice: effects on reticuloendothelial function and tissue distribution. *J Pharmacol Exp Ther* **229:**267–275.

Burhop K, Gordon D, and Estep T (2004) Review of hemoglobin-induced myocardial lesions. *Artif Cells Blood Substit Immobil Biotechnol* **32:**353–374.

Chen JY, Scerbo M, and Kramer G (2009) A review of blood substitutes: examining the history, clinical trial results, and ethics of hemoglobin-based oxygen carriers. *Clinics (Sao Paulo)* **64:**803–813.

Clavijo-Alvarez JA, Sims CA, Pinsky MR, and Puyana JC (2005) Monitoring skeletal muscle and subcutaneous tissue acid-base status and oxygenation during hemorrhagic shock and resuscitation. *Shock* **24:**270–275.

Dams ET, Laverman P, Oyen WJ, Storm G, Scherphof GL, van Der Meer JW, Corstens FH, and Boerman OC (2000) Accelerated blood clearance and altered biodistribution of repeated injections of sterically stabilized liposomes. *J Pharmacol Exp Ther* **292:**1071–1079.

Demoy M, Andreux JP, Weingarten C, Gouritin B, Guilloux V, and Couvreur P (1999) Spleen capture of nanoparticles: influence of animal species and surface characteristics. *Pharm Res* **16:**37–41.

Fernández-Urrusuno R, Fattal E, Rodrigues JM Jr, Féger J, Bedossa P, and Couvreur P (1996) Effect of polymeric nanoparticle administration on the clearance activity of the mononuclear phagocyte system in mice. *J Biomed Mater Res* **31:**401–408.

Goins B, Klipper R, Sanders J, Cliff RO, Rudolph AS, and Phillips WT (1995) Physiological responses, organ distribution, and circulation kinetics in anesthetized rats after hypovolemic exchange transfusion with technetium-99m-labeled liposome-encapsulated hemoglobin. *Shock* **4:**121–130.

Hunt JP, Hunter CT, Brownstein MR, Ku J, Roberts L, Currin RT, Lemasters JJ, and Baker CC (2001) Alteration in Kupffer cell function after mild hemorrhagic shock. *Shock* **15:**403–407.

Ishida T, Ichihara M, Wang X, and Kiwada H (2006a) Spleen plays an important role in the induction of accelerated blood clearance of PEGylated liposomes. *J Control Release* **115:** 243–250.

Ishida T, Ichihara M, Wang X, Yamamoto K, Kimura J, Majima E, and Kiwada H (2006b) Injection of PEGylated liposomes in rats elicits PEG-specific IgM, which is responsible for rapid elimination of a second dose of PEGylated liposomes. *J Control Release* **112:**15–25.

Ishida T and Kiwada H (2008) Accelerated blood clearance (ABC) phenomenon upon repeated injection of PEGylated liposomes. *Int J Pharm* **354:**56–62.
Ishida T, Masuda K, Ichikawa T, Ichihara M, Irimura K, and Kiwada H (2003) Accelerated clearance of a second injection of PEGylated liposomes in mice. *Int J Pharm* **255:**167–174.
Ishida T, Wang X, Shimizu T, Nawata K, and Kiwada H (2007) PEGylated liposomes elicit an anti-PEG IgM response in a T cell-independent manner. *J Control Release* **122:**349–355.
Jaeschke H, Farhood A, Bautista AP, Spolarics Z, and Spitzer JJ (1993) Complement activates Kupffer cells and neutrophils during reperfusion after hepatic ischemia. *Am J Physiol* **264:** G801–G809.
Jahr JS, Moallempour M, and Lim JC (2008) HBOC-201, hemoglobin glutamer-250 (bovine), Hemopure (Biopure Corporation). *Expert Opin Biol Ther* **8:**1425–1433.
Kuebler JF, Toth B, Yokoyama Y, Bland KI, Rue LW 3rd, and Chaudry IH (2004) α_1-Acid-glycoprotein protects against trauma-hemorrhagic shock. *J Surg Res* **119:**21–28.
Laverman P, Carstens MG, Boerman OC, Dams ET, Oyen WJ, van Rooijen N, Corstens FH, and Storm G (2001) Factors affecting the accelerated blood clearance of polyethylene glycol-liposomes upon repeated injection. *J Pharmacol Exp Ther* **298:**607–612.
Martin F, Oliver AM, and Kearney JF (2001) Marginal zone and B1 B cells unite in the early response against T-independent blood-borne particulate antigens. *Immunity* **14:**617–629.
Mayer MM (1961) Complement and complement fixation, in *Kabat and Mayer's Experimental Immunochemistry,* 2nd ed (Kabat EA ed) pp 133–240, Charles C Thomas, Springfield.
Natanson C, Kern SJ, Lurie P, Banks SM, and Wolfe SM (2008) Cell-free hemoglobin-based blood substitutes and risk of myocardial infarction and death: a meta-analysis. *JAMA* **299:** 2304–2312.
Rymsa B, Wang JF, and de Groot H (1991) O_2^- release by activated Kupffer cells upon hypoxia-reoxygenation. *Am J Physiol* **261:**G602–G607.
Sakai H, Hara H, Yuasa M, Tsai AG, Takeoka S, Tsuchida E, and Intaglietta M (2000) Molecular dimensions of Hb-based O_2 carriers determine constriction of resistance arteries and hypertension. *Am J Physiol Heart Circ Physiol* **279:**H908–H915.
Sakai H, Horinouchi H, Tomiyama K, Ikeda E, Takeoka S, Kobayashi K, and Tsuchida E (2001) Hemoglobin-vesicles as oxygen carriers: influence on phagocytic activity and histopathological changes in reticuloendothelial system. *Am J Pathol* **159:**1079–1088.
Sakai H, Masada Y, Horinouchi H, Ikeda E, Sou K, Takeoka S, Suematsu M, Takaori M, Kobayashi K, and Tsuchida E (2004a) Physiological capacity of the reticuloendothelial system for the degradation of hemoglobin vesicles (artificial oxygen carriers) after massive intravenous doses by daily repeated infusions for 14 days. *J Pharmacol Exp Ther* **311:**874–884.
Sakai H, Masada Y, Horinouchi H, Yamamoto M, Ikeda E, Takeoka S, Kobayashi K, and Tsuchida E (2004b) Hemoglobin-vesicles suspended in recombinant human serum albumin for resuscitation from hemorrhagic shock in anesthetized rats. *Crit Care Med* **32:**539–545.
Sakai H, Seishi Y, Obata Y, Takeoka S, Horinouichi H, Tsuchida E, and Kobayashi K (2009) Fluid resuscitation with artificial oxygen carriers in hemorrhaged rats: profiles of hemoglobin-vesicle degradation and hematopoiesis for 14 days. *Shock* **31:**192–200.
Sakai H, Takeoka S, Park SI, Kose T, Nishide H, Izumi Y, Yoshizu A, Kobayashi K, and Tsuchida E (1997) Surface modification of hemoglobin vesicles with poly(ethylene glycol) and effects on aggregation, viscosity, and blood flow during 90% exchange transfusion in anesthetized rats. *Bioconjug Chem* **8:**23–30.
Sakai H, Tomiyama K, Masada Y, Takeoka S, Horinouchi H, Kobayashi K, and Tsuchida E (2003) Pretreatment of serum containing hemoglobin vesicles (oxygen carriers) to prevent their interference in laboratory tests. *Clin Chem Lab Med* **41:**222–231.
Sakai H and Tsuchida E (2007) Hemoglobin-vesicles for a transfusion alternative and targeted oxygen delivery. *J Liposome Res* **17:**227–235.
Smani Y (2008) Hemospan: a hemoglobin-based oxygen carrier for potential use as a blood substitute and for the potential treatment of critical limb ischemia. *Curr Opin Investig Drugs* **9:**1009–1019.
Sou K, Klipper R, Goins B, Tsuchida E, and Phillips WT (2005) Circulation kinetics and organ distribution of Hb-vesicles developed as a red blood cell substitute. *J Pharmacol Exp Ther* **312:**702–709.
Sou K and Tsuchida E (2008) Electrostatic interactions and complement activation on the surface of phospholipid vesicle containing acidic lipids: effect of the structure of acidic groups. *Biochim Biophys Acta* **1778:**1035–1041.
Taguchi K, Maruyama T, Iwao Y, Sakai H, Kobayashi K, Horinouchi H, Tsuchida E, Kai T, and Otagiri M (2009a) Pharmacokinetics of single and repeated injection of hemoglobin-vesicles in hemorrhagic shock rat model. *J Control Release* **136:**232–239.
Taguchi K, Miyasato M, Watanabe H, Sakai H, Tsuchida E, Horinouchi H, Kobayashi K, Maruyama T, and Otagiri M (2010) Alteration in the pharmacokinetics of hemoglobin-vesicles in a rat model of chronic liver cirrhosis is associated with Kupffer cell phagocyte activity. *J Pharm Sci* doi:10.1002/jps.22286.
Taguchi K, Urata Y, Anraku M, Maruyama T, Watanabe H, Sakai H, Horinouchi H, Kobayashi K, Tsuchida E, Kai T, et al. (2009b) Pharmacokinetic study of enclosed hemoglobin and outer lipid component after the administration of hemoglobin vesicles as an artificial oxygen carrier. *Drug Metab Dispos* **37:**1456–1463.
Taguchi K, Urata Y, Anraku M, Watanabe H, Kadowaki D, Sakai H, Horinouchi H, Kobayashi K, Tsuchida E, Maruyama T, et al. (2009c) Hemoglobin vesicles, polyethylene glycol (PEG)ylated liposomes developed as a red blood cell substitute, do not induce the accelerated blood clearance phenomenon in mice. *Drug Metab Dispos* **37:**2197–2203.
Tsuchida E, Sou K, Nakagawa A, Sakai H, Komatsu T, and Kobayashi K (2009) Artificial oxygen carriers, hemoglobin vesicles and albumin-hemes, based on bioconjugate chemistry. *Bioconjug Chem* **20:**1419–1440.
Wang X, Ishida T, and Kiwada H (2007) Anti-PEG IgM elicited by injection of liposomes is involved in the enhanced blood clearance of a subsequent dose of PEGylated liposomes. *J Control Release* **119:**236–244.
Yamaoka K, Tanigawara Y, Nakagawa T, and Uno T (1981) A pharmacokinetic analysis program (multi) for microcomputer. *J Pharmacobiodyn* **4:**879–885.

Address correspondence to: Dr. Masaki Otagiri, Department of Biopharmaceutics, Graduate School of Pharmaceutical Sciences, Kumamoto University, 5-1 Oe-honmachi, Kumamoto 862-0973, Japan. E-mail: otagirim@gpo.kumamoto-u.ac.jp

Journal of Controlled Release 148 (2010) 373–379

Contents lists available at ScienceDirect

Journal of Controlled Release

journal homepage: www.elsevier.com/locate/jconrel

NANOMEDICINE

Release abilities of adenosine diphosphate from phospholipid vesicles with different membrane properties and their hemostatic effects as a platelet substitute

Yosuke Okamura [a,c], Shunsuke Katsuno [a], Hidenori Suzuki [b], Hitomi Maruyama [c], Makoto Handa [c], Yasuo Ikeda [a], Shinji Takeoka [a,*]

[a] Department of Life Science and Medical Bioscience, Graduate School of Advanced Science and Engineering, Waseda University, TWIns, Tokyo 162-8480, Japan
[b] Center for Electron Microscopy, the Tokyo Metropolitan Institute of Medical Science, Tokyo 156-8506, Japan
[c] Department of Transfusion Medicine & Cell Therapy, Keio University, Tokyo 160-8582, Japan

ARTICLE INFO

Article history:
Received 27 March 2010
Accepted 14 September 2010
Available online 25 September 2010

Keywords:
Platelet substitute
Phospholipid vesicles
Controlled release
Adenosine 5'-diphosphate (ADP)
Membrane flexibility
Lamellarity

ABSTRACT

We have constructed phospholipid vesicles with hemostatic activity as a platelet substitute. The vesicles were conjugated with a dodecapeptide (HHLGGAKQAGDV, H12), which is a fibrinogen γ-chain carboxy-terminal sequence (γ400–411). We have recently exploited these vesicles as a potential drug delivery system by encapsulation of adenosine 5'-diphosphate (ADP) (H12-(ADP)-vesicles).

Here we explore the relationship between the ADP release from H12-(ADP)-vesicles with different membrane properties and their hemostatic effects. In total, we prepared five kinds of H12-(ADP)-vesicles with different lamellarities and membrane flexibilities. By radioisotope-labeling, we directly show that H12-(ADP)-vesicles were capable of augmenting platelet aggregation by releasing ADP in an aggregation-dependent manner. The amount of ADP released from the vesicles was dependent on their membrane properties. Specifically, the amount of ADP released increased with decreasing lamellarity and tended to increase with increasing membrane flexibility. Our *in vivo* results clearly demonstrated that H12-(ADP)-vesicles with the ability to release ADP exert considerable hemostatic action in terms of correcting prolonged bleeding time in a busulphan-induced thrombocytopenic rat model.

We propose a recipe to control the hemostatic abilities of H12-(ADP)-vesicles by modulating ADP release based on membrane properties. We believe that this concept will be invaluable to the development of platelet substitutes and other drug carriers.

1. Introduction

Transfusion of platelet concentrates by blood donation is currently the only means of effectively treating bleeding caused by quantitative platelet disorders. In particular, the supply of platelet concentrate is always an issue because of its short shelf life (4 days in Japan, 5–7 days in the United States and Europe). Moreover, the risk of blood-borne infections, such as bacterial sepsis, and acute immune reactions remains a major concern for allogeneic platelet transfusion [1,2]. For these reasons, a number of trials have been conducted to develop platelet substitutes (artificial platelets) reproducing platelet functions and working synergistically with activated platelets such as infusible platelet membranes (IPMs) [3], fibrinogen-bonded red blood cells [4], fibrinogen-bearing liposomes [5], fibrinogen-coated albumin microcapsules (Synthocyte) [6] and arginine-glycine-asparaginic acid (RGD) peptide-bound red blood cells (Thromboerythrocytes) [7]. These platelet substitutes consist of materials derived from blood components and micrometer sized carriers.

Glycoprotein (GP) IIb/IIIa, which exists on the membrane of platelets, changes its form from inactive to active when platelets adhere to collagen exposed on sites of vascular injury [8,9]. In the circulation, platelet aggregation is mediated by fibrinogen by bridging adjacent platelets through GPIIb/IIIa in an activation-dependent manner. A dodecapeptide HHLGGAKQAGDV (H12), corresponding to the fibrinogen γ-chain carboxy-terminal sequence (γ400–411), is a specific binding site of the ligand for activated GPIIb/IIIa [10,11].

Our strategy for the development of platelet substitutes relies on the fact that biocompatible and biodegradable nanocarriers, such as phospholipid vesicles [12–15] and polymerized albumin particles [16–18], specifically accumulate at sites of vascular injury by virtue of their own mass. We aimed to construct a carrier that would accumulate with the activated GPIIb/IIIa. With this in mind, we conjugated the H12 sequence to these carriers [19] because isolated human fibrinogen is unstable [20]. As anticipated, the H12-conjugated vesicles specifically accumulated at sites of vascular injury in the tail vein using computed tomography [15]. Moreover, these vesicles dose-dependently corrected the bleeding time in rats with moderate thrombocytopenia *in vivo* [14].

* Corresponding author. Tel./fax: +81 3 5369 7324.
E-mail address: takeoka@waseda.jp (S. Takeoka).

0168-3659/$ – see front matter © 2010 Elsevier B.V. All rights reserved.
doi:10.1016/j.jconrel.2010.09.013

Adenosine 5'-diphosphate (ADP) is a physiologically relevant platelet agonist that is stored in dense granules of the platelet. Upon platelet activation ADP is released and functions to reinforce or maintain platelet aggregation through corresponding platelet nucleotide receptors $P2Y_1$ and $P2Y_{12}$. ADP itself is a weak agonist, but synergizes the effects of other agonists even at suboptimal concentrations [21]. Moreover, ADP also stabilizes aggregates formed by strong agonists such as thrombin [22].

In order to strengthen the hemostatic ability of H12-vesicles as a platelet substitute, we have recently developed a drug delivery function by encapsulating ADP into vesicles (H12-(ADP)-vesicles). In fact, the H12-(ADP)-vesicles exhibited considerable hemostatic ability for correcting prolonged bleeding time in a busulphan-induced thrombocytopenic rat model [23]. However, we have indirectly demonstrated the release of encapsulated contents from vesicles using a fluorescent probe in place of ADP.

Here, we aimed to explore the relationship between ADP release from the H12-(ADP)-vesicles and their hemostatic characteristics. We prepared five kinds of H12-(ADP)-vesicles, each with different membrane flexibilities and lamellarities, and then directly measured ADP release by radioisotope-labeling of ADP and cholesterol as a membrane component. Furthermore, we intravenously infused H12-(ADP)-vesicles into thrombocytopenic rats and measured the tail bleeding time in order to evaluate the hemostatic ability of the vesicle preparations.

2. Materials and methods

2.1. Materials

1,2-Dimyristoyl-*sn*-glycero-3-phosphatidylcholine (DMPC), 1,2-dipalmitoyl-*sn*-glycero-3-phosphatidylcholine (DPPC), 1,2-distearoyl-*sn*-glycero-3-phosphatidylcholine (DSPC) and cholesterol were purchased from Nippon Fine Chemical Co., Ltd. (Osaka, Japan). 1,2-Distearoyl-*sn*-glycero-3-phosphatidylethanolamine-*N*-[monomethoxypoly(ethyleneglycol)] (PEG-DSPE, 5.1 kDa) was from NOF Co. (Tokyo, Japan). 1,5-Dihexadecyl-*N*-succinyl-L-glutamate (DHSG) [24] and H12-PEG-Glu2C18, where H12 carrying cysteine at the N-terminal was conjugated with maleimide group at the end of the PEG-lipids [14], were synthesized in our laboratory. Adenosine 5'-diphosphate (ADP) and prostaglandin E_1 (PGE_1) were purchased from Sigma-Aldrich (St Louis, MO). Rabbit anti-H12 antibody (1.1 mg/mL) was synthesized by Oriental Yeast Co., Ltd. (Tokyo, Japan). [8-^{14}C]ADP (3.7 MBq/mL) and [1,2-^{3}H]cholesterol (37 MBq/mL) were purchased from Moravek Biochemicals Inc. (Brea, CA) and American Radiolabeled Chemicals Inc. (St Louis, MO), respectively. Solvable™ and Hionic-Fluor™ were purchased from PerkinElmer Japan Co., Ltd. (Yokohama, Japan). Dioctadecyloxacarbocyanine perchlorate ($DiOC_{18}$), which is a fluorescent dye for vesicles and is often used for visualization of the disordered area of lipid membrane [25], and thrombin receptor activator peptide-6 amide trifluoroacetate salt (TRAP) were purchased from Invitrogen (Eugene, OR) and Bachem AG (Bubendorf, Switzerland), respectively. Sephadex G25 for gel permeation chromatography (GPC) was purchased from GE Healthcare (Amersham, UK). Busulphan and poly(ethylene glycol) (400 Da) were purchased from Sigma-Aldrich. Sevofrane was purchased from Maruishi Pharmaceutical Co. (Osaka, Japan).

2.2. Preparation of H12-(ADP)-vesicles

DMPC (92 mg, 136 μmol, gel-to-liquid crystalline phase transition temperature (T_c) of the multilamellar vesicles of the pure lipid: 24 °C), cholesterol (52.7 mg, 136 μmol), DHSG (18.9 mg, 27.2 μmol), PEG-DSPE (5.2 mg, 0.90 μmol) and H12-PEG-Glu2C18 (4.7 mg, 0.90 μmol) were dissolved in benzene and then freeze-dried. The resulting lipid mixture was hydrated with phosphate-buffered saline (PBS) (pH 7.4) containing 1 mM ADP for 3 h at room temperature (RT) and extruded using membrane filters with pore sizes of 0.45, 0.22 or 0.20 μm (Durapore®; Millipore Co., Tokyo) at 4 °C or RT for control of their lamellarities. Instead of DMPC, DPPC (100 mg, 136 μmol, T_c: 41 °C) and other lipids were also freeze-dried and then hydrated with 1 mM ADP solution for 3 h at RT. The preparations were extruded using membrane filters with pore sizes of 0.45, 0.22 or 0.20 μm at RT or 60 °C. Likewise, DSPC (107 mg, 136 μmol, T_c: 54 °C) and other lipids were freeze-dried and hydrated with 1 mM ADP solution for 3 h at RT. Samples were then extruded with membrane filters with pore sizes of 0.45, 0.22 or 0.20 μm at RT. Five kinds of vesicles were washed with PBS by centrifugation (100,000 *g*, 30 min, 4 °C), and the unencapsulated ADP was eliminated by GPC. Particle diameter was analyzed using a dynamic light-scattering method (N4 PLUS; Beckman-Coulter, Fullerton, FL).

2.3. Preparation of H12-(ADP)-vesicles labeled with ^{3}H-cholesterol and ^{14}C-ADP

We prepared radioisotope-labeled H12-(ADP)-vesicles, referred to as H12-(^{14}C-ADP)-(^{3}H-vesicles), using essentially the same procedure as described above. During the hydration process the mixed lipids were hydrated with PBS containing 1 mM ADP and [8-^{14}C]ADP (1.85 MBq) for 3 h before extrusion with membrane filters of pore size 0.45, 0.22 or 0.20 μm. The vesicles were washed with PBS by centrifugation (100,000 *g*, 30 min, 4 °C) for removal of the remaining ADP. Next, [1,2-^{3}H]cholesterol in ethanol (1.85 MBq) was added to the resulting vesicle suspension and incubated at RT for 10 min. Finally, unincorporated [1,2-^{3}H]cholesterol and ADP were eliminated by GPC in order to obtain the purified H12-(^{14}C-ADP)-(^{3}H-vesicles).

2.4. Calculation of lamellarity of the H12-(ADP)-vesicles

Lamellarity, the average number of bilayer membrane of the vesicle, was calculated from the volume ratio of vesicles in the dispersion. The vesicle dispersion ([lipid] = final concentration (fc), 0.9 mg/mL) was mixed with a PEG solution (M_w = 100 kDa, fc, 10 mg/mL) and precipitated by hematocrit centrifugation to measure the volume ratio of vesicles. Lamellarity (N) was calculated by Eq. (1),

$$N = \frac{AVC \times 10^{-3}}{2S \times R \times 10^{-8}} \quad (1)$$

where, volume and the surface area of vesicle are V (m^3) and S (m^2), respectively, and the volume ratio of vesicles in the dispersion, lipid concentration, and the molecular area of lipid are R (%), C (M), and A (m^2), respectively.

2.5. Retention of ADP encapsulated into the H12-(ADP)-vesicles

Retention of ADP encapsulated into vesicles was measured as follows. The H12-(ADP)-vesicles at a lipid concentration of 10 mg/mL were incubated at 37 °C and collected at various time intervals. After separation on GPC, the fraction of H12-(ADP)-vesicles was collected. The vesicles were dissolved by adding 2% (v/v) deca(oxyethylene) dodecyl ether (fc, 1 % (v/v)), and the solution was heated at 50 °C for 5 min for complete dissolution of the vesicles. The ADP was quantified by high pressure liquid chromatography (HPLC) on a TSK-GEL ODS-100 V column (TOSOH Co. (Tokyo); 4.6 mm o.d. × 250 mm h) using a mobile phase of 97% (v/v) phosphoric acid (pH 7.0) and 3% (v/v) methanol containing 30 mM triethylamine at 1 mL/min and the detection wavelength of 260 nm. Moreover, the ADP encapsulation ratio was corrected for lipid concentration, which was quantified

using a phospholipid test kit (Wako Pure Chemical Industries Ltd., Osaka).

2.6. Flow cytometric analyses

Blood withdrawn from healthy volunteers was mixed with 10% volume of 3.8% (w/v) sodium citrate. Platelet-rich plasma (PRP) was prepared by centrifugation of the blood (100 *g*, 15 min, RT). PRP was mixed with a 15% volume of acid-citrate-dextrose solution composed of 2.2% (w/v) sodium citrate, 0.8% (w/v) citric acid, and 2.2% (w/v) glucose (ACD) containing 1 μM PGE_1. The suspension was centrifuged (2200 *g*, 7 min, RT), and the plasma was replaced with a Ringer's-citrate-dextrose solution (RCD solution, composition: 0.76% (w/v) citric acid, 0.090% (w/v) glucose, 0.043% (w/v) $MgCl_2$, 0.038% (w/v) KCl, 0.60% (w/v) NaCl, pH 6.5) containing 1 μM PGE_1. The platelet pellets were carefully resuspended in the RCD solution, and then the suspension was centrifuged (2200 *g*, 7 min, RT). Finally, the resulting platelet pellets were resuspended in a Hepes-Tyrode buffer (H-T buffer, pH 7.4). The platelet count was adjusted to 1.0×10^5/μL using an automated hematology analyzer (K-4500; Sysmex Co., Kobe, Japan).

A solution of $DiOC_{18}$ in DMSO (2 mM, 50 μL) was added to the dispersion of the five kinds of H12-(ADP)-vesicles (20 mg/mL, 5 mL), which was then incubated for 10 min at RT. The free $DiOC_{18}$ was eliminated by GPC to collect the $DiOC_{18}$-labeled H12-(ADP)-vesicles. The dispersion of the $DiOC_{18}$-labeled H12-(ADP)-vesicles (9 mg/mL, 10 μL) was added to the platelet suspension ([platelet] = 1.0×10^5/μL, 50 μL). TRAP (fc, 50 μM) was then mixed with the suspension to activate the platelets and incubated at 37 °C for 10 min before being fixed with formaldehyde (fc, 1.5% (v/v)). We also performed the same experiments for the three different control (ADP)-vesicles. The platelets were gated to their characteristic forward vs. side scatter, and 10,000 platelets were analyzed using a FACSCalibur flow cytometer (Nihon Becton Dickinson, Co., Tokyo). The number of platelets binding with the H12-(ADP)-vesicles was quantified as a fraction of the fluorescent-positive platelets. Each experiment was performed at least three times.

2.7. Platelet aggregation studies and ADP release measurements

The platelet count of the PRP was adjusted to 2.0×10^5/μL using platelet-poor plasma (PPP), which was prepared by centrifugation of the citrated blood (2200 *g*, 10 min, RT). An ADP solution (fc, 3 μM) was added to the PRP containing H12-(ADP)-vesicles (fc, 0.10–0.30 mg/mL), and light transmittance was measured using an aggregometer (Hema Tracer T-638; Nico Bioscience, Tokyo, Japan).

Platelet aggregation studies of H12-(^{14}C-ADP)-(^{3}H-vesicles) were also performed under the same conditions (37 °C, 5 min) in order to measure the percentage of ADP release from the vesicles. Samples were fixed with formaldehyde (fc, 1.5% (v/v)) 5 min after measurement. The percentage ADP release from vesicles was measured as follows. PRP containing H12-(^{14}C-ADP)-(^{3}H-vesicles) was dissolved with solvable™ (2 mL) and then Hionic Fluor™ (15 mL) was added. The disintegration per minute (DPM) of ^{3}H and ^{14}C, which were defined as A_{3H} and A_{14C}, respectively, was measured using a liquid scintillation analyzer (TRI-CARB 3100TR; PerkinElmer Japan Co., Ltd.). For the aggregation studies, the suspension was stirred for 5 min after ADP stimulation and then centrifuged (5000 *g*, 5 min, 4 °C) to obtain the platelet aggregates. The aggregates were subsequently washed with PBS (5000 *g*, 5 min, 4 °C) to separate the remaining vesicles. The resulting aggregates were also dissolved and the DPM of ^{3}H and ^{14}C in the aggregates, defined as B_{3H} and B_{14C}, measured. The platelet pellet after 5 min stirring without ADP stimulation was also collected by centrifugation (5000 *g*, 5 min, 4 °C). The DPM of ^{3}H and ^{14}C in the pellet, which were defined as C_{3H} and C_{14C}, respectively, was then measured. We defined "co-sediment ratio of vesicles with platelet aggregation (%)" and "ADP release from vesicles (%)" using the following equations:

$$\text{Co-sediment ratio of vesicles with platelet aggregation}(\%) = \frac{B_{3H}-C_{3H}}{A_{3H}} \times 100$$

$$\text{ADP release from vesicles}(\%) = \frac{\frac{A_{14C}}{A_{3H}}(B_{3H}-C_{3H})-(B_{14C}-C_{14C})}{\frac{A_{14C}}{A_{3H}}(B_{3H}-C_{3H})} \times 100$$

2.8. Immunogold electron microscopy of H12-(ADP)-vesicles and aggregated platelets

For observation of H12-(ADP)-vesicles involved in platelet aggregates, the platelet reaction triggered with ADP was terminated by the addition of an equal volume (200 μL) of 0.4% (w/v) glutaraldehyde in 0.1 M phosphate buffer (PB, pH 7.4) and the platelets were fixed at 4 °C for 30 min. After the mixture was transferred to 1.5 mL microtubes, the fixed platelets were sedimented by centrifugation at 756 *g* for 3 min at 4 °C. The platelet pellets were cut into small pieces and rinsed with 0.1 M PB twice and then with 0.01 M PBS (pH 7.2) three times at 4 °C.

Ultrathin frozen sections were obtained essentially using the procedure described by Tokuyasu [26] with slight modifications [27]. The fixed platelets were sequentially immersed in 1 M sucrose in PBS for 60 min, 1.84 M sucrose in PBS for 2 h and then 1.84 M sucrose and 20% (w/v) polyvinylpyrolidone (M_w: 10 kDa) in PBS overnight at 4 °C. After freezing the platelets in liquid nitrogen, ultrathin frozen sections were cut using an ultramicrotome (Ultracut, Reichert, Vienna, Austria) with a cryo-attachment (FC-4E, Reichert) at −90 °C and then the sections were mounted on nickel grids. The grids were floated on a drop of PBS to rinse the mounted sections and then transferred onto a drop of 0.5% (w/v) bovine serum albumin in PBS for blocking. The sections were incubated with rabbit anti-H12 antibody (0.22 μg/mL in PBS) overnight at 4 °C. After the sections were rinsed five times with PBS, they were incubated with goat anti-rabbit IgG coupled to colloidal gold (10 nm, 1:50 final dilution; GE HealthCare) for 60 min at RT. After the sections were rinsed with PBS three times and distilled water five times, they were stained with uranyl acetate. Regions of platelet aggregates and vesicles in the stained sections were examined with a JEM 1200EX electron microscope (JEOL Ltd., Tokyo) at an acceleration voltage of 80 kV.

Table 1
Characterization of vesicles ($n=3$).

Vesicles[a]	H12-PEG-Glu2C18	Diameter (nm)	Lamellality (−)
1	+	240±68	1.1±0.1
2	+	285±78	1.1±0.2
3	+	298±107	1.2±0.2
1'	+	240±70	1.9±0.5[b]
2'	+	287±83	1.8±0.3[b]
1"	−	270±82	1.1±0.2
2"	−	272±69	1.1±0.2
3"	−	280±76	1.2±0.1

[a] **1**: DMPC/cholesterol/DHSG/H12-PEG-Glu2C18/PEG-DSPE = 5/5/1/0.03/0.03, **2**: DPPC/ cholesterol/DHSG/H12-PEG-Glu2C18/PEG-DSPE = 5/5/1/0.03/0.03, **3**: DSPC/ cholesterol/DHSG/H12-PEG-Glu2C18/PEG-DSPE = 5/5/1/0.03/0.03. **1'** and **2'** show **1** and **2** with multilamellarities, respectively. **1"**, **2"**, and **3"** show **1**, **2**, and **3** lacking H12-PEG-Glu2C18, respectively.

[b] $P<0.05$ vs. control vesicle **1"** or vesicle **2"**.

Table 2
Co-sediment ratio of vesicles into platelet aggregates and release of ADP from vesicles ($n=4$).

Vesicles	Co-sediment ratio of vesicles into platelet aggregates (%)	ADP release from vesicles (%)
1	9.5±1.2*	58.8±6.1*†
2	10.8±2.3*	49.9±5.0*†
3	8.3±1.1*	0
1'	11.3±3.1*	24.5±4.2*
2'	13.3±1.0*	21.2±6.9*
1"	0.7±0.8	0
2"	0.1±0.2	0
3"	0.0±0.2	0

*$P<0.05$ vs. control vesicles **1"**, **2"**, or **3"** , respectively. †$P<0.05$ vs. multilamellar vesicles **1'** or **2'**, respectively. #$P<0.05$ vs. vesicles **3**.

2.9. Preparation of busulphan-induced thrombocytopenic rats and measurement of tail bleeding time

Animal studies were approved by the Animal Subject Committee of Keio University School of Medicine and performed in accordance with the NIH guideline for laboratory animals. Busulphan-induced thrombocytopenic rats were prepared as described previously [14,16]. Briefly, male Wistar rats (230–250 g; Sankyo Labo Service Co., Tokyo) were anesthetized with diethyl ether and injected on Day 0 and Day 3 with 10 mg/kg, for a total dosage of 20 mg/kg of busulphan. On Day 10, thrombocytopenic rats were anesthetized with sevofrane, and the sample suspension at a dose of 4 mL/kg was infused into the tail vein. After 5 min, a 2.5 mm (length)×1.0 mm (depth) template-guided incision (Quikheel™; Becton-Dickinson Co., San Jose, CA) was made 1 cm from the tip of the tail. The tail was immersed in a 50 mL cylinder of saline, and the time required for bleeding to stop was measured.

2.10. Statistical analyses

All values are reported as mean±standard deviation. Statistical analyses for Tables 1 and 2 were compared using the Student's unpaired t test. Statistical significance of data for the H12-(ADP)-vesicle group compared with saline groups was tested using Tukey–Kramer tests (Fig. 6). P-values of less than 0.05 were considered statistically significant. Statistical analyses were performed using StatView software (HULINKS Inc., Tokyo).

3. Results and discussion

3.1. Characterization of the H12-(ADP)-vesicles

We prepared three kinds of unilamellar H12-(ADP)-vesicles with different membrane flexibilities (**1**: DMPC/cholesterol/DHSG=5/5/1, **2**: DPPC/cholesterol/DHSG=5/5/1, and **3**: DSPC/cholesterol/DHSG=5/5/1, by molar ratios) and two kinds of multilamellar H12-(ADP)-vesicles (**1'**: DMPC/cholesterol/DHSG=5/5/1, and **2'**: DPPC/cholesterol/DHSG=5/5/1). These surfaces were modified with 0.3 mol% PEG-DSPE and 0.3 mol% H12-PEG-Glu2C18. ADP at 1 mM, as optimized previously, was encapsulated in the inner space of the vesicles [23]. Furthermore, we also prepared the three kinds of unilamellar control (ADP)-vesicles without H12-PEG-Glu2C18 (**1"**: DMPC/cholesterol/DHSG=5/5/1, **2"**: DPPC/cholesterol/DHSG=5/5/1, and **3"**: DSPC/cholesterol/DHSG=5/5/1).

When the lipid dispersion of **1** was extruded at 4 °C and the lipid dispersions of **2** and **3** were extruded at RT, the lamellarities of the resulting vesicles of **1–3** were calculated to be 1.1±0.1, 1.1±0.2, and 1.2±0.2, respectively. Moreover, in this way, the diameters of the vesicles could also be controlled (see Table 1). By contrast, when the lipid dispersions of **1'** and **2'** were extruded at RT or 60 °C, the lamellarities of the resulting vesicles of **1'** and **2'** were calculated to be 1.9±0.5 and 1.8±0.3, respectively (Table 1). These results show that lamellarities of the vesicles could be controlled by considering the gel-to-liquid crystalline phase transition temperature (T_c) of the main lipid components such as DMPC, DPPC and DSPC. Of course, although their T_c disappeared by introduction of cholesterol, the membrane flexibilities were obviously different as shown in our previous demonstration based on the fluorescent depolarization method [13,28]. It is suggested that when the extrusion temperature is near T_c of the PCs or higher, the multilamellar membranes could deform their shape and cleave easily during passing of the vesicles through the pores of the membrane filters, leading to the smaller vesicles with a relatively high lamellarity. On the other hand, when the extrusion temperature is lower than T_c, the higher pressure is necessary for the vesicles in order to pass through the pores. This would lead to form the smaller vesicles with a lower lamellarity. In fact, electron microscopic images of the vesicles **1–3** in the ultrathin frozen sections showed spherical unilamellar vesicles (Fig. 1). Vesicles **1'** and **2'** were identified as being multilamellar (Fig. 1). Furthermore, H12 on the surface of the vesicles was detected by the immunogold method using anti-H12 antibody, suggesting that the H12 molecules were homogenously bound on the surface of the vesicles. Unfortunately, we could not prepare multilamellar DSPC-based H12-(ADP)-vesicles because encapsulated ADP was degraded at temperatures exceeding 70 °C (data not shown). We also prepared unilamellar control vesicles **1"–3"** in a similar manner using an extrusion temperature of 4 °C, RT and RT, respectively. Furthermore, the endotoxin contamination in the vesicle suspensions at a lipid concentration of 10 mg/mL was below 0.25 EU/mL. This was considered acceptable for *in vivo* studies.

3.2. Binding of the H12-(ADP)-vesicles towards the activated platelets

We studied the binding abilities of the H12-(ADP)-vesicles with different membrane flexibilities or lamellarities to the activated platelets by FACS analyses. The $DiOC_{18}$-labeled H12-(ADP)-vesicles **1–3, 1'** and **2'** did not bind to the resting platelets in suspension (Fig. 2). For the TRAP-stimulated platelets, the H12-(ADP)-vesicles **1–3, 1'** and **2'** displayed significant binding. Furthermore, the binding ratios were found to be comparable. In the presence of PAC-1, which recognizes an epitope on the GPIIb/IIIa complex of activated platelets [29], the binding of the H12-(ADP)-vesicles to the stimulated platelets was significantly inhibited (data not shown). This indicates that all H12-(ADP)-vesicles specifically interacted with the activated platelets and their binding abilities were unaffected by membrane flexibility.

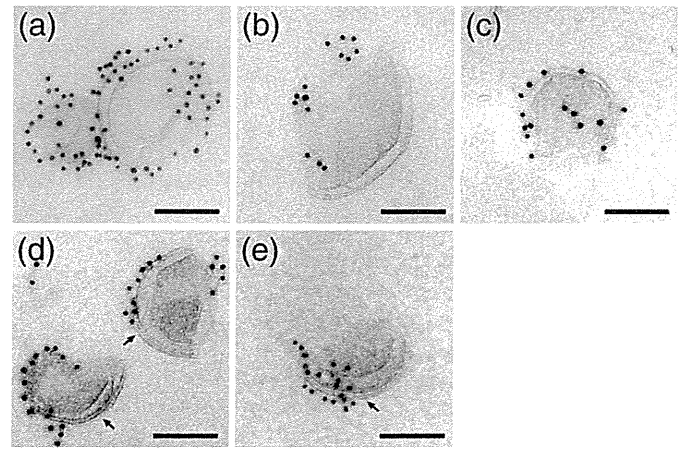

Fig. 1. Electron micrographs of the H12-(ADP)-vesicles ((a) vesicle **1**, (b) vesicle **2**, (c) vesicle **3**, (d) vesicle **1'**, and (e) vesicle **2'**). Membranes of vesicles **1**, **2** and **3** show a unilamellar structure, and those of vesicles **1'** and **2'** are identified as multilamellar (arrows). Gold labels for H12 are distributed on the surface of the vesicles, respectively. Scale bars show 100 nm.

3.3. Function of the H12-(ADP)-vesicles for platelet aggregation

We evaluated effects of the vesicles on ADP-induced platelet aggregation. When PBS was added to PRP, the maximum light transmittance of platelet aggregation induced at a suboptimal ADP concentration of 3 μM was 34±4% (n=3) (Fig. 3). This was comparable to that of control (ADP)-vesicles **1"–3"** and control vesicles without ADP (average maximum transmittance: 33±5% (n=3)) (data not shown). The maximum transmittance of vesicles **3** was slightly increased to 38±4% (n=3). When vesicles **1** and **2** were added instead, platelet aggregation significantly increased to 54±4 and 51±5%, respectively (n=3). In case of the multilamellar vesicles **1'** and **2'**, the maximum transmittances of 46±3 and 42±5% were lower than those of vesicles **1** and **2**, although higher than that of vesicles **3** (n=3). None of the H12-(ADP)-vesicles caused platelet aggregation in the absence of ADP stimulation (data not shown). These results suggest that H12-conjugated vesicles with encapsulated ADP that had a low level of lamellarity can augment platelet aggregation significantly and the vesicles with higher membrane flexibilities tend to be augmented platelet aggregation. Specifically, the order of the platelet aggregation effect induced by the vesicles was **1**≈**2**>**1'**≈**2'**>**3**.

To explore whether the augmented aggregation effect of H12-(ADP)-vesicles is dependent on the amount of ADP released from the vesicles, we prepared radioisotope-labeled H12-(ADP)-vesicles (H12-(^{14}C-ADP)-(^{3}H-vesicles)). ^{14}C-ADP was used to distinguish ADP encapsulated into vesicles from that stored intrinsically in dense granules of the platelets. Based on the equation shown in Materials and methods, we calculated the co-sedimentation ratios of various H12-(^{14}C-ADP)-(^{3}H-vesicles) with platelet aggregates and ADP release ratios from the vesicles (Table 2).

By comparison with the (^{14}C-ADP)-(^{3}H-vesicles) **1"–3"** (**1"**: 0.7±0.8%, **2"**: 0.1±0.2%, **3"**: 0.0±0.2%) as control, significant amounts of vesicles **1–3** (**1**: 9.5±1.2%, **2**: 10.8±2.3%, **3**: 8.3±1.1%) became specifically associated with platelet aggregates (n=4). However, ADP was not released from vesicle **3** or any of the control vesicles **1"–3"** (n=4), suggesting that under physiological condition (37 °C), the membrane flexibility of the vesicles **3** should be low in comparison with that of other vesicles and the vesicles **3** would be difficult to deform even after interacting with platelets in our previous demonstration based on the fluorescent depolarization method [28]. When vesicles **1** and **2** were used instead, ADP was readily released (**1**: 58.8±6.1% and **2**: 49.9±5.0%), and the amount of ADP release tended to increase with increasing membrane flexibility (n=4). These observations suggest that the amount of ADP released from H12-vesicles is influenced by their membrane deformability (see later). A significant amount (**1'**: 11.3±3.1%, **2'**: 13.3±1.0%) of multilamellar vesicles **1'** and **2'** also became specifically associated with platelet aggregates in comparison with control vesicles. Indeed, the amount of association was comparable to those of vesicles **1–3** (n=4). However, the ADP release percentages from vesicles **1'** and **2'** were reduced by half (**1'**: 24.5±4.2%, **2'** 21.2±6.9%) (n=4) in comparison with unilamellar vesicles **1** and **2**. These results show that the amount of ADP released from H12-vesicles was also significantly dependent on their lamellarities. Specifically, the amount of ADP released from vesicles increased in the following order **1**≈**2**>**1'**≈**2'**>**3**, which also corresponds to the order of the augmented aggregation effect induced by the vesicles (Fig. 3).

The H12-(ADP)-vesicles **1–3** involved in platelet aggregates could be identified by immunogold electron microscopy. Platelet aggregates formed in the presence of vesicle **3** were smaller than those of vesicles **1** and **2** as judged by the transmittance of the platelet aggregates. The vesicles gave electron-lucent images in which H12 was identified on the surface by labeling with colloidal gold. In all cases, vesicles were

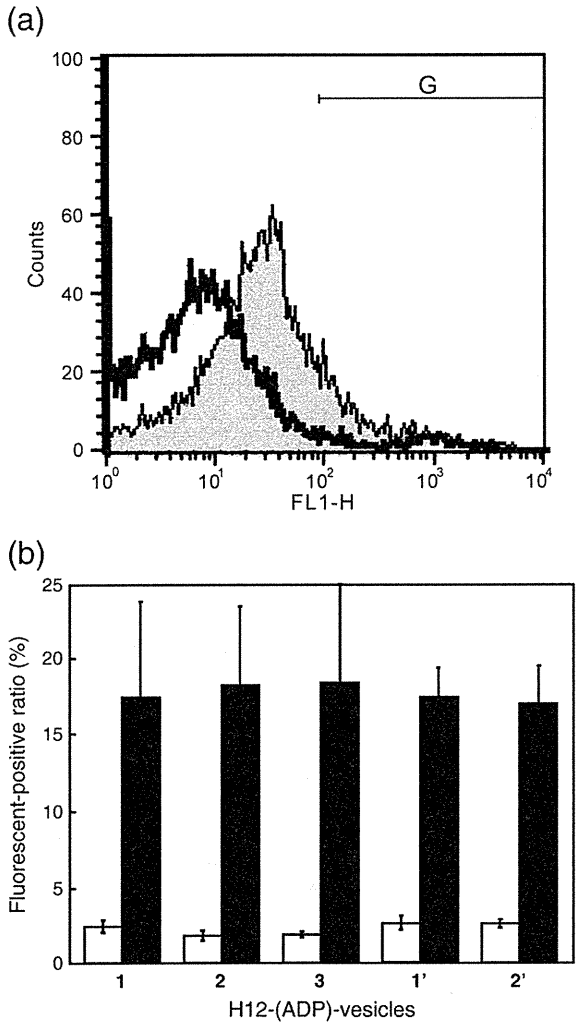

Fig. 2. Specific interactions of H12-(ADP)-vesicles **1–3**, **1'** and **2'** with TRAP-stimulated platelets using flow cytometry. (a) The solid histogram shows representative data of TRAP-stimulated platelets stained with $DiOC_{18}$-labeled H12-(ADP)-vesicles; blank histogram represents resting platelets in the presence of $DiOC_{18}$-labeled H12-(ADP)-vesicles. (b) The bar graph summarizes the percentage fluorescent positive platelets quantified as a fraction "G" as shown in (a). Experiments were performed in triplicate. White and block columns denote binding of H12-(ADP)-vesicles to resting and TRAP-stimulated platelets, respectively.

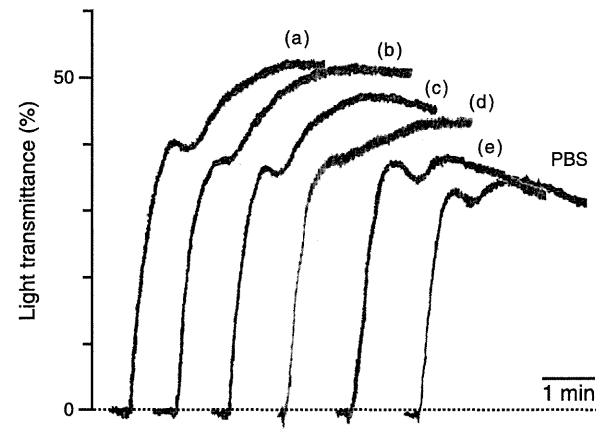

Fig. 3. Augmentation of ADP-induced platelet aggregation by H12-(ADP)-vesicles. Aggregation measurement in PRP ([platelet]=2.0×10^5/μL) obtained from a healthy volunteer in the presence of (a) vesicle **1**, (b) vesicle **2**, (c) vesicle **1'**, (d) vesicle **2'**, or (e) vesicle **3**. Traces are representative of data obtained from at least three independent experiments. Vesicle concentration and ADP administration were fc, 0.15–0.30 mg/mL and fc, 3 μM, respectively.

associated with the plasma membrane of the activated platelets and between adherent platelets (Fig. 4). Intriguingly, irregular-shaped vesicles labeled with colloidal gold were observed between the adherent platelets, suggesting that some vesicles lose their round structures (deformability) and the part of the vesicles might have a possibility to disrupt after association with the platelets. Based on these results, aggregation-dependent ADP release from H12-vesicles may be caused by the following mechanism. Vesicles incorporated into the platelet aggregates are subject to physical forces, such as compression, in the gap between adherent platelets. As a direct consequence of these forces, the vesicle shape is transformed from round to indeterminate. The degree of shape change (deformability including a possibility to disrupt) is dependent on their membrane flexibilities and lamellarities, which is correlated with the amount of ADP released from the vesicles.

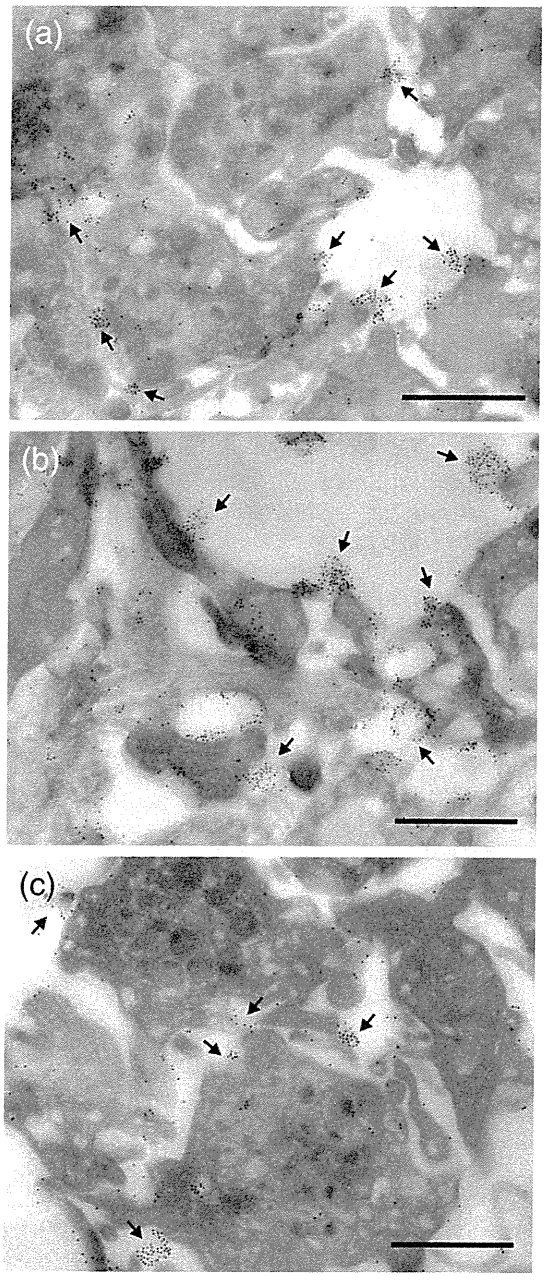

Fig. 4. Electron micrographs of the platelet aggregates involving the H12-(ADP)-vesicles ((a) vesicle **1**, (b) vesicle **2**, and (c) vesicle **3**). The vesicles detected by colloidal gold for H12 were distributed on the platelet surface and between adherent platelets (arrows). Scale bars show 1 μm.

3.4. Stability of ADP encapsulated into the H12-(ADP)-vesicles

Prior to the *in vivo* studies, we explored the stability of ADP encapsulated in the H12-(ADP)-vesicles. H12-(ADP)-vesicle **2** and **3** lost none of their encapsulated ADP after seven days incubation at 37 °C ($n=3$) (Fig. 5). Indeed, the same result was found after seven days incubation at 60 °C (data not shown), equivalent to an incubation period of seven years at 4 °C. However, when the H12-(ADP)-vesicles **1** were incubated at 37 °C, the encapsulated ADP gradually leaked from the vesicles and the amount of encapsulated ADP was reduced by half after seven days. These results indicate that vesicle **1** with higher membrane flexibility had lower encapsulation stability for ADP under the same set of storage conditions. However, ADP was easily released from vesicle **1** in a platelet aggregation-dependent manner. Consequently, we tested the *in vivo* hemostatic effect of vesicles **2** and **3** except vesicles **1**, which did and did not have the ability to release ADP, respectively.

3.5. Hemostatic effects of H12-(ADP)-vesicles on tail bleeding time in thrombocytopenic rats

In order to clarify whether ADP release from the H12-(ADP)-vesicles could be effective for *in vivo* hemostatic ability, a rat model with busulphan-induced thrombocytopenia was prepared. Tail bleeding times of normal (platelet count, $8.1\pm0.8\times10^5/\mu L$) and thrombocytopenic rats ($1.7\pm1.3\times10^5/\mu L$) 5 min after intravenous infusion of saline were 178 ± 56 s and 711 ± 189 s ($n=7$), respectively (Fig. 6). Bleeding times of thrombocytopenic rats after infusion of H12-vesicles without ADP (the same component as vesicle **2**) at doses of 10 and 40 mg/kg were 573 ± 143 s and 335 ± 98 s ($n=9$), respectively. This data confirms our previous finding of a dose-dependent hemostatic effect of H12-vesicles in a rat model [14]. We further showed that H12-vesicles specifically accumulate at sites of vascular injury. In fact, using a CT analysis, we recently demonstrated that the H12-vesicles containing iopamidol as a contrast dye was specifically concentrated at the site of an injured vein in the tail of the rat [15].

Infusion of H12-(ADP)-vesicles **2** at 4 mg/kg, which had the ability to release ADP, reduced bleeding time slightly to 521 ± 88 s ($n=10$). Increasing doses of H12-(ADP)-vesicles **2** at 10 and 40 mg/kg significantly corrected the bleeding time to 349 ± 49 s and 397 ± 102 s ($n=10$), respectively. In particular, shortening of the bleeding time by vesicle **2** at a dose of 10 mg/kg almost corresponded to that observed for H12-vesicles at a dose of 40 mg/kg. By contrast, infusion of H12-(ADP)-vesicle **3**, which did not release ADP, at doses of 10 mg/kg gave a bleeding time of 650 ± 189 s ($n=10$). These results are comparable to those of the saline control group. Increasing the dose to

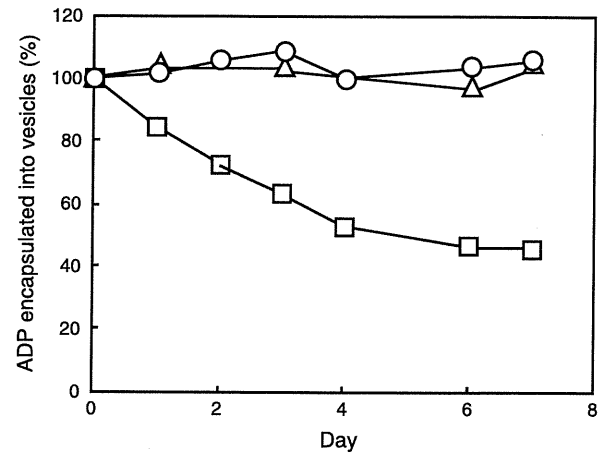

Fig. 5. Stability of ADP encapsulated into the H12-(ADP)-vesicles incubated at a temperature of 37 °C. (□) vesicle **1**, (Δ) vesicle **2**, and (○) vesicle **3**.

40 mg/kg resulted in a reduction in bleeding time to 453 ± 100 s ($n = 10$), comparable with the findings obtained using H12-vesicles without ADP. Unfortunately, we could not obtain the data on the differences between vesicles **2** and vesicles **3** at a higher dose (40 mg/kg), though both vesicles significantly corrected the bleeding time in comparison with the saline control group. However, we confirmed previously that vesicles **2** at higher dose corrected the bleeding time of rabbits with severe thrombocytopenia (platelet count: $2.1 \pm 0.5 \times 10^4/\mu L$) dose-dependently [23]. These results suggest that hemostatic effect of vesicles should be strongly influenced by the ratio between the dosage of vesicles and platelet counts in animals. However, our *in vivo* results clearly demonstrate that ADP encapsulation into H12-vesicles brings about a local release of ADP from the vesicles at the site of vascular injury. Consequently, the hemostatic effects were successfully augmented in the thrombocytopenic rat model.

In conclusion, we succeeded in preparation of H12-(ADP)-vesicles with various membrane flexibilities, of which lamellarities could be controlled by considering the T_c of the main lipid component during extrusion. Using the resulting vesicles, we propose a recipe to control the hemostatic ability of H12-(ADP)-vesicles by controlling ADP release from the vesicles. Such controlled release of ADP is based on membrane deformability i.e., membrane flexibility and lamellarity. Furthermore, we believe that the novel procedure described in this paper will aid in the successful development of platelet substitutes and other drug carriers.

Acknowledgments

The authors wish to thank Drs. N. Watanabe, K. Yokoyama and M. Murata at Keio University for the valuable discussion. This work was supported in part by Health and Labor Sciences Research Grants (Research on Pharmaceutical and Medical Safety, H.S., M.H., Y.I. and S.T.), Ministry of Health, Labor and Welfare, Japan. Y.O. was the recipient of a Research Fellowships from the Japan Health Sciences Foundation.

References

[1] S.J. Slichter, Platelet transfusion therapy, Hematol. Oncol. Clin. North Am. 21 (2007) 697–729.
[2] D.F. Stroncek, P. Rebulla, Platelet transfusions, Lancet 370 (2007) 427–438.
[3] S.S. Graham, N.J. Gonchoroff, J.L. Miller, Infusible platelet membranes retain partial functionality of the platelet GPIb/IX/V receptor complex, Am. J. Clin. Pathol. 115 (2001) 144–147.

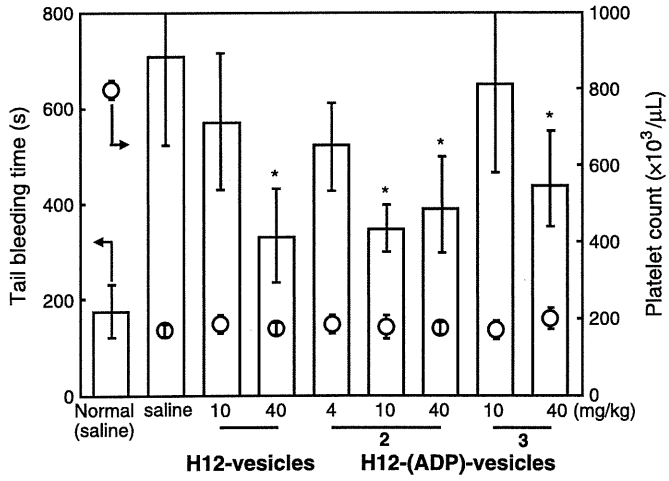

Fig. 6. Hemostatic effects of H12-(ADP)-vesicles on rat tail bleeding time (white column). ○, platelet count in rats ($n = 6$–10). *$P<0.05$ for H12-(ADP)-vesicles or H12-vesicles group vs. saline group.

[4] G. Agam, A.A. Livine, Erythrocytes with covalently bound fibrinogen as a cellular replacement for the treatment of thrombocytopenia, Eur. J. Clin. Invest. 22 (1992) 105–112.
[5] E. Casals, A. Verdaguer, R. Tonda, A. Galan, G. Escolar, J. Estelrich, Atomic force microscopy of liposomes bearing fibrinogen, Bioconjug. Chem. 14 (2003) 593–600.
[6] M. Levi, P.W. Friedrich, S. Middleton, P.G. De Groot, Y.P. Wu, R. Harris, B.J. Biemond, F.G. Heijien, J. Levin, J.W. Ten Cate, Fibrinogen-coated albumin microcapsules reduce bleeding in severely thrombocytopenic rabbits, Nat. Med. 5 (1999) 107–111.
[7] B.S. Coller, K.T. Springer, J.H. Beer, N. Mohandas, L.E. Scudder, K.J. Norton, S.M. West, Thromboerythrocytes. In vitro studies of a potential autologous, semi-artificial alternative to platelet transfusion, J. Clin. Invest. 89 (1992) 546–555.
[8] J. Takagi, B.M. Petre, T. Walz, T.A. Springer, Global comformational rearrangemrents in integrin extracellular domains in outside-in and inside-out signaling, Cell 110 (2002) 599–611.
[9] T. Xiao, J. Takagi, B.S. Coller, J.H. Wang, T.A. Springer, Structual basis for allostery in integrins and binding to fibrinogen-mimetic therapeutics, Nature 432 (2004) 59–67.
[10] S.C. Lam, E.F. Plow, M.A. Smith, A. Andrieux, J.J. Ryckwaert, G. Marguerie, M.H. Ginsberg, Evidence that arginyl-glycyl-aspartate peptides and fibrinogen γ chain peptides share a common binding site on platelets, J. Biol. Chem. 262 (1987) 947–950.
[11] A. Andrieux, G. Hudry-Clergeon, J.J. Ryckewaert, A. Chapel, M.H. Ginsberg, E.F. Plow, G. Marguerie, Amino acid sequences in fibrinogen mediating its interaction with its platelet receptor, GPIIbIIIa, J. Biol. Chem. 264 (1989) 9258–9265.
[12] T. Kitaguchi, M. Murata, K. Iijima, K. Kamide, T. Imagawa, Y. Ikeda, Characterization of liposomes carrying von Willebrand factor-binding domain of platelet glycoprotein Ibα: A potential substitute for platelet transfusion, Biochem. Biophys. Res. Commun. 261 (1999) 784–789.
[13] S. Takeoka, Y. Teramura, Y. Okamura, M. Handa, Y. Ikeda, E. Tsuchida, Rolling properties of rGPIbα-conjugated phospholipid vesicles with different membrane flexibility on the vWf surface under flow conditions, Biochem. Biophys. Res. Commun. 296 (2002) 765–770.
[14] Y. Okamura, I. Maekawa, Y. Teramura, H. Maruyama, H. Handa, Y. Ikeda, S. Takeoka, Hemostatic effects of phospholipid vesicles carrying fibrinogen-γ chain dodecapeptide in vitro and in vivo, Bioconjug. Chem. 16 (2005) 1589–1596.
[15] Y. Okamura, K. Eto, H. Maruyama, M. Handa, Y. Ikeda, S. Takeoka, Visualization of liposomes carrying fibrinogen γ-chain dodecapeptide accumulated to sites of vascular injury using computed tomography, Nanomedicine 6 (2010) 391–396.
[16] Y. Okamura, S. Takeoka, Y. Teramura, H. Maruyama, E. Tsuchida, M. Handa, Y. Ikeda, Hemostatic effects of fibrinogen γ-chain dodecapeptide-conjugated polymerized albumin particles in vitro and in vivo, Transfusion 45 (2005) 1221–1228.
[17] Y. Okamura, T. Fujie, H. Maruyama, M. Handa, Y. Ikeda, S. Takeoka, Prolonged hemostatic ability of poly(ethylene glycol)-modified polymerized albumin particles carrying fibrinogen γ-chain dodecapeptide, Transfusion 47 (2007) 1254–1262.
[18] Y. Okamura, T. Fujie, M. Nogawa, H. Maruyama, Y. Handa, S. Ikeda, Takeoka, Hemostatic effects of polymerized albumin particles carrying fibrinogen γ-chain dodecapeptide as platelet substitutes in severely thrombocytopenic rabbits, Transf. Med. 18 (2008) 158–166.
[19] S. Takeoka, Y. Okamura, Y. Teramura, N. Watanabe, H. Suzuki, E. Tsuchida, M. Handa, Y. Ikeda, Function of fibrinogen γ-chain dodecapeptide-conjugated latex beads under flow, Biochem. Biophys. Res. Commun. 312 (2003) 773–779.
[20] S. Takeoka, Y. Teramura, Y. Okamura, M. Handa, Y. Ikeda, E. Tsuchida, Fibrinogen-conjugated albumin polymers and their interaction with platelets under flow conditions, Biomacromolecules 2 (2001) 1192–1197.
[21] J.A. Ware, M. Smith, E.W. Salzman, Synergism of platelet-aggregating agents. Role of elevation of cytoplasmic calcium, J. Clin. Invest. 80 (1987) 267–271.
[22] M. Cattaneo, M.T. Canciani, A. Lecchi, R.L. Kinlough-Rathbone, M.A. Packham, P.M. Mannucci, J.F. Mustard, Released adenosine diphosphate stabilizes thrombin-induced human platelet aggregates, Blood 75 (1990) 1081–1086.
[23] Y. Okamura, S. Takeoka, K. Eto, I. Maekawa, T. Fujie, H. Maruyama, Y. Ikeda, M. Handa, Development of fibrinogen γ-chain peptide-coated, adenosine 5'-diphosphate-encapsulated liposomes as a synthetic platelet substitute, J. Thromb. Haemost. 7 (2009) 470–477.
[24] S. Takeoka, K. Mori, H. Ohkawa, K. Sou, E. Tsuchida, Synthesis and assembly of poly (ethylene glycol)-lipids with mono-, di-, tetraacyl chains and a poly(ethylene glycol) chain of various molecular weights, J. Am. Chem. Soc. 122 (2000) 7927–7935.
[25] D.C. Carrer, A.W. Schmidt, H.J. Knolker, P. Schwille, Membrane domain-disrupting effects of 4-substitued cholesterol derivatives, Langmuir 24 (2008) 8807–8812.
[26] K.T. Tokuyasu, Use of poly(vinylpyrrolidone) and poly(vinylalcohol) for cryoultramicrotomy, Histochem. J. 21 (1989) 163–171.
[27] H. Suzuki, S. Nakamura, Y. Itoh, T. Tanaka, H. Yamazaki, K. Tanoue, Immunocytochemical evidence for the translocation of α-granule membrane glycoprotein IIb/IIIa (integrin αIIbβ3) of human platelets to the surface membrane during the release reaction, Histochemistry 97 (1992) 381–388.
[28] S. Takeoka, T. Ogushi, K. Terase, T. Ohmori, E. Tsuchida, Layer-controlled hemoglobin vesicles by interaction of hemoglobin with a phospholipid assembly, Langmuir 12 (1996) 1755–1759.
[29] R. Taub, R.J. Gould, V.M. Garsky, T.M. Ciccarone, J. Hoxie, P.A. Friedman, S.J. Shattil, A monoclonal antibody aganst the platelet fibrinogen reseptor contains a sequence that mimics a receptor recognition domein receptor, J. Biol. Chem. 264 (1989) 259–265.

POTENTIAL CLINICAL RELEVANCE

Nanomedicine: Nanotechnology, Biology, and Medicine 6 (2010) 391–396

nanomedicine

ELSEVIER

Original Article

www.nanomedjournal.com

Visualization of liposomes carrying fibrinogen γ-chain dodecapeptide accumulated to sites of vascular injury using computed tomography

Yosuke Okamura, PhD[a,b], Kaoruko Eto, MS[a], Hitomi Maruyama, BS[b], Makoto Handa, MD, PhD[b], Yasuo Ikeda, MD, PhD[a], Shinji Takeoka, PhD[a,*]

[a]*Department of Life Science and Medical Bioscience, Graduate School of Advanced Science and Engineering, Waseda University, TWIns, Tokyo, Japan*
[b]*Department of Transfusion Medicine and Cell Therapy, School of Medicine, Keio University, Tokyo, Japan*

Received 29 November 2008; accepted 13 July 2009

Abstract

We have constructed liposomes with hemostatic activity as a platelet substitute using moderately thrombocytopenic rats. The liposomes were conjugated with the dodecapeptide (HHLGGAKQAGDV: H12), which is a fibrinogen γ-chain C-terminal sequence (γ 400–411). To visualize liposome accumulation at the site of vascular injury by in vivo computed tomography, a water-soluble contrast dye, *N,N′*-bis[2-hydroxy-1-(hydroxylmethyl)ethyl]-5-[(2*S*)-2-hydroxylpropanoylamino]-2,4,6-triiodoisophthalamide (iopamidol), was encapsulated into the H12-conjugated liposomes. We achieved direct visualization of specific accumulation of the H12-(iopamidol)liposomes at the jugular vein injured by ferric chloride and succeeded in semiquantitative analyses of the accumulated amount of H12-liposomes in the injured site. We therefore propose that H12-liposomes that are specifically recruited to, and exert their hemostatic activity at the site of vascular injury, have a significant potential as a carrier and/or as an ideal platelet substitute. Furthermore, the H12-(iopamidol)liposomes would also be clinically useful as diagnostic agents for pathological thrombus detection and as contrast dyes for hepatosplenography.

From the Clinical Editor: The authors have constructed liposomes with hemostatic activity as a platelet substitute using moderately thrombocytopenic rats. They propose that H12-liposomes that are specifically recruited to, and exert their hemostatic activity at the site of vascular injury, have a significant potential as a carrier and/or as an ideal platelet substitute. Furthermore, the H12-(iopamidol) liposomes would also be clinically useful as diagnostic agents for thrombus detection and as contrast dyes for hepatosplenography.

Key words: Platelet substitute; Dodecapeptide; Liposome; Iopamidol; Computed tomography

Platelet transfusion has an important function in supportive therapy for patients with thrombocytopenia caused by hematological malignancies, or as a result of intensive chemotherapy and radiation therapy for cancer. However, the shortage of platelet concentrates has always been a serious issue because of short shelf-life (4 days in Japan), insufficient donation, the risk of viral and bacterial infections, as well as alloimmunization associated with transfusion. For these reasons several trials have been conducted to develop platelet substitutes (artificial platelets) reproducing platelet functions such as infusible platelet membranes,[1] solubilized platelet membrane protein-conjugated liposomes (plateletsomes),[2] fibrinogen-bonded red blood cells,[3] fibrinogen-bearing liposomes,[4] fibrinogen-coated albumin microcapsules (synthocytes),[5] and arginine-glycine-asparaginic acid (RGD) peptide-bound red blood cells (thromboerythrocytes).[6] These platelet substitutes consist of materials derived from blood components.

Glycoprotein (GP) IIb/IIIa, which exists on the platelet membrane, changes from an inactive to an active form when platelets adhere to collagen exposed on sites of vascular injury.[7,8] The activated GPIIb/IIIa acts as a receptor for fibrinogen and von Willebrand factor,[9,10] which leads to platelet aggregation.[11] A dodecapeptide HHLGGAKQAGDV (H12), corresponding to the fibrinogen γ-chain C-terminal sequence (γ 400–411), is a specific binding site of the ligand for activated GPIIb/IIIa.[12]

This work was supported by Health and Labor Sciences Research Grants (Research on Pharmaceutical and Medical Safety, M.H., Y.I., and S.T.), Ministry of Health, Labor and Welfare, Japan. Y.O. was the recipient of Japan Health Sciences Foundation.

*Corresponding author. Department of Life Science and Medical Bioscience, Graduate School of Advanced Science and Engineering, Waseda University, TWIns, Tokyo, Japan.

E-mail address: takeoka@waseda.jp (S. Takeoka).

1549-9634/$ – see front matter © 2010 Elsevier Inc. All rights reserved.
doi:10.1016/j.nano.2009.07.004